

Compressive sensing meets time-frequency: An overview of recent advances in time-frequency processing of sparse signals

Ervin Sejdić^a, Irena Orović^b, Srdjan Stanković^b

^a*Department of Electrical and Computer Engineering, Swanson School of Engineering, University of Pittsburgh, Pittsburgh, PA, 15261, USA*

^b*Faculty of Electrical Engineering, University of Montenegro, Podgorica, Montenegro*

Abstract

Compressive sensing is a framework for acquiring sparse signals at sub-Nyquist rates. Once compressively acquired, many signals need to be processed using advanced techniques such as time-frequency representations. Hence, we overview recent advances dealing with time-frequency processing of sparse signals acquired using compressive sensing approaches. The paper is geared towards signal processing practitioners and we emphasize practical aspects of these algorithms. First, we briefly review the idea of compressive sensing. Second, we review two major approaches for compressive sensing in the time-frequency domain. Thirdly, compressive sensing based time-frequency representations are reviewed followed by descriptions of compressive sensing approaches based on the polynomial Fourier transform and the short-time Fourier transform. Lastly, we provide brief conclusions along with several future directions for this field.

Keywords:

Compressive sensing, time-frequency analysis, time-frequency dictionary, nonstationary signals, sparse signals

1. Introduction

Time-frequency analysis provides a framework for a descriptive analysis of non-stationary signals whose models are not available or easily constructed [1], [2]. For such signals, time or frequency domain descriptions typically do not offer comprehensive details about changes in signal characteristics [3]. The main issue with the time domain representation is that it provides no details about the frequency content of those signals, and sometimes, even the time content can be difficult to interpret [4]. The frequency domain on

8 the other hand provides no easily understood timing details about the occurrence of vari-
9 ous frequency components [5]. In other words, timing details are buried within the phase
10 spectrum of a signal, which is the most common reason for only analyzing the amplitude
11 spectrum of a signal obtained via the Fourier transform. To combine timing and spectral
12 into a joint representation, a time variable is typically introduced into a Fourier-based
13 analysis to obtain two-dimensional, redundant representations of non-stationary signals
14 [6]. Such representation provide a description of spectral signal changes as a function
15 of time, that is, the description of time-varying energy concentration changes along the
16 frequency axis. In an ideal case, these two-dimensional signal representations would com-
17 bine instantenous frequency spectrum with global temporal behavior of a signal [7], [8],
18 [9],[10], [11], [12], [13], [14], [15].

19 Time-frequency analysis is often employed in the analysis of complex non-stationary
20 signals (e.g., physiological signals [16], [17], [18], [19], [20], [21], [22], [23], mechanical
21 vibrations [24], [25], [26], [27], audio signals [28], [29], [30], radar signals [31], [32], [33],
22 [34], [35], [36]). However, continuously monitoring such signals for an extended period
23 of time can impose heavy burdens on data acquisition and processing systems, even
24 when sampling these non-stationary signals at low sampling rates. To avoid these data
25 acquisition and processing burdens, compressive sensing aims to compress signals during
26 a data acquisition process, rather than afterwards [37], [38], [39], [40], [41], [42], [43], [44],
27 [45], [46], [47], [48], [49], [50], [51], [52].

28 In this paper, we review recent advances that combine the ideas of time-frequency
29 and compressive sensing analyses. Section 2 reviews the main ideas behind compres-
30 sive sensing. In Section 3, we introduce the main approaches to obtain compressed
31 samples in the time-frequency domain. Several different approaches are presented here
32 including compressive sensing in the ambiguity domain, but also compressive sensing of
33 non-stationary signals using time-frequency dictionaries. We also reviewed compressive
34 sensing approaches that relied on the short-time Fourier transform and the polynomial
35 Fourier transform. Compressive sensing based time-frequency representations are de-
36 scribed in Section 4. Conclusions and future directions are provided in Section 5.

37 2. Compressive Sensing

38 In traditional signal processing, the Shannon-Nyquist sampling theorem mandates
39 that any signal needs to be sampled at least twice the highest frequency present in the
40 signal to be able to accurately recover information present in the signal. The traditional
41 sampling approach can yield a large number of samples, and compressive strategies are
42 often used immediately after sampling in order to reduce storage requirements or trans-
43 mission complexities. While this has been a prevailing approach for many years, it is
44 clearly a redundant approach as most of acquired samples are disregarded immediately
45 after sampling. To avoid these redundant steps, compressive sensing has been proposed
46 and it postulates a signal can be recovered using a fewer number of samples than required
47 by the Shannon-Nyquist theorem [38], [39], [53], [40], [54] [55], [56], [57], [58], [59], [60],
48 [61], [62], [63].

49 The main idea behind compressive sensing is to combine sensing and compression steps
50 into a single step during a data acquisition process [39], [40], [42], [64], [65]. Compressive
51 sensing approaches typically acquire signals at sub-Nyquist rates (e.g., one tenth of the
52 Nyquist rate) and signals can be accurately recovered from these samples with *a certain*
53 *probability* [39]. These approaches work very well for K -sparse signals, i.e., signals that
54 can be represented by K bases in an N -dimensional space. In other words, compressive
55 sensing approaches will acquire $M \ll N$ samples that will encode a K -sparse signal of
56 dimension N by computing a measurement vector \mathbf{y} of a signal vector \mathbf{s} [66], [67], [68],
57 [69]:

$$\mathbf{y} = \Phi \mathbf{s} \tag{1}$$

58 where Φ represents an $M \times N$ sensing matrix [40]. The signal vector \mathbf{s} can be recovered
59 from sparse samples by utilizing a norm minimization approach:

$$\min \|\mathbf{s}\|_0 \text{ subject to } \|\mathbf{y} - \Phi \mathbf{s}\|_2 < \xi \tag{2}$$

60 where ξ is measurement noise, $\|\mathbf{s}\|_0$ represents the number of nonzero entries of \mathbf{s} and
61 $\|\bullet\|_2$ is the Euclidian norm. However, it should be mentioned that it is not guaranteed
62 that eqns. (1) and (2) will provide an accurate representation of sparse signals. In some
63 applications that are sensitive to small changes such as medical diagnostic applications, it

64 is almost mandatory to achieve almost perfect recovery of these sparse signals, otherwise
 65 compressive sensing schemes are not useful at all in medical diagnostic applications.
 66 To reach these almost perfect reconstructions of sparse signals, compressive sensing can
 67 be performed in other domains (i.e., other than the time domain), which yields a new
 68 reformulation of the compressive sensing approach proposed in (1) as [64], [67]:

$$\mathbf{y} = \mathbf{\Phi}\mathbf{s} = \mathbf{\Phi}\mathbf{\Psi}\mathbf{x}. \quad (3)$$

69 Here, \mathbf{x} is the vector of expansion coefficients representing the sparse representation of
 70 the signal \mathbf{s} in the basis $\mathbf{\Psi}$. A very good example of this change is representing a single
 71 sinusoid in the frequency domain. This transformation would enable us to represent
 72 such a sinusoid with by a two-sparse vector. In this paper, this change of the domain
 73 is achieved by representing a signal in the time-frequency domain, rather than using its
 74 time-domain samples.

75 It should be understood that the compressive sensing approach proposed by eqn. (3)
 76 affects the sparsity in the transform domain, which then inherently affects the number
 77 of measurements needed to reconstruct a signal. This is assessed using the so-called
 78 coherence measure between the matrices $\mathbf{\Phi}$ and $\mathbf{\Psi}$ [70], [71], [72], [73]:

$$\mu(\mathbf{\Phi}, \mathbf{\Psi}) = \sqrt{N} \max |\langle \phi_k, \psi_j \rangle| \quad (4)$$

79 where N is the signal length, ϕ_k is the k^{th} row of $\mathbf{\Phi}$, and ψ_j is the j^{th} row of $\mathbf{\Psi}$. Smaller
 80 values of the coherence measure typically denote that a smaller number of random mea-
 81 surements is needed to accurately reconstruct a signal.

82 **3. Time-frequency based compressive sensing**

83 The time-frequency domain represent an ideal domain to sparsely represent nonsta-
 84 tionary signals for several different reasons. First, it is very difficult to represent nonsta-
 85 tionary signals sparsely either in time or frequency domains. For example, a frequency
 86 modulated signal is concentrated along its instantaneous frequency in the time-frequency
 87 domain, and most of other values are equal to zero. But, its frequency domain repre-
 88 sentation has many non-zero components, and its time domain representation typically
 89 has many (large) amplitude changes that can be difficult to compress. Therefore, such a

90 frequency modulated signal or any other signal with complex non-stationary structures
 91 should be compressively sampled in the time-frequency domain, as their representations
 92 are often sparse in the time-frequency domain [74], [75], [76]. Second, recent advances in
 93 computational resources enabled fast manipulations of large matrices, which are required
 94 for compressive sensing of nonstationary signals in the time-frequency domain [77].

95 In this section, we will overview two major approaches for compressive sensing of
 96 nonstationary signals in the time-frequency domain. We will begin with compressively
 97 sampling a nonstationary signal in the ambiguity domain as proposed in [78] with un-
 98 derstanding that this approach is only applicable for quadratic time-frequency represen-
 99 tations. A more general approach is to utilize time-frequency dictionaries to obtain a
 100 sparse time-frequency representation of a nonstationary signal, which can be then used
 101 to compressively sensed such a signal.

102 3.1. Compressive sensing in the ambiguity domain

103 As mentioned in the previous paragraph, the ambiguity domain provides a suitable
 104 framework to compressively sampled non-stationary signals. To achieve representations
 105 in the ambiguity domain, we can start with the Wigner-Ville distribution, $WVD(t, f)$,
 106 and take the two-dimensional Fourier transform of it to obtain the ambiguity domain
 107 representation [1], [79]:

$$A_x(\nu, \tau) = \mathcal{F}_{2D}\{WVD(t, f)\} \quad (5)$$

108 where \mathcal{F}_{2D} is the forward and inverse two-dimensional Fourier operator. The ambibility
 109 domain offers an opportunity to suppress or completely remove cross-terms, which plague
 110 the quadratic time-frequency representations, as cross-terms are typically displaced from
 111 the origin in the ambiguity domain, and the auto-terms are typically centered around the
 112 origin. Therefore, low-pass filtering by multiplying the ambiguity representation of the
 113 signal, $A_x(\nu, \tau)$, by a kernel function $k(\nu, \tau)$:

$$\mathcal{A}_x(\nu, \tau) = A_x(\nu, \tau)k(\nu, \tau). \quad (6)$$

114 However, it should be mentioned here that compressive sensing approaches here are
 115 mostly used to obtain enhanced time-frequency signal energy localization in the time-
 116 frequency domain. Specifically, we compressively sample the ambiguity domain repre-
 117 sentation of the signal in order to obtain a very sparse time-frequency domain signal

118 representation. This is achieved by solving the l_1 -norm minimization problem to obtain
 119 a sparse time-frequency distribution $\widehat{\Upsilon}_x(t, f)$:

$$\widehat{\Upsilon}_x(t, f) = \arg \min_{\Upsilon_x(t, f)} \|\Upsilon_x(t, f)\|_1 \quad (7)$$

$$F_{2D}\{\Upsilon_x(t, f)\} - \mathcal{A}_x^M = 0|_{(\nu, \tau) \in \Omega} \quad (8)$$

120 where \mathcal{A}_x^M denotes the set of samples from the ambiguity domain in the region defined by
 121 the mask $(\nu, \tau) \in \Omega$, $\Upsilon_x(t, f)$ denotes the time-frequency distribution, and $\|\cdot\|_1$ denotes
 122 the ℓ_1 norm. Noise distributions can be approximated as follows:

$$\widehat{\Upsilon}_x(t, f) = \arg \min_{\Upsilon_x(t, f)} \|\Upsilon_x(t, f)\|_1 \quad (9)$$

$$\|F_{2D}\{\Upsilon_x(t, f)\} - \mathcal{A}_x^M\|_2 \leq \epsilon|_{(\nu, \tau) \in \Omega} \quad (10)$$

123 One has to carefully select samples in the ambiguity domain via an appropriate ambiguity
 124 function masking, which is formed as a small, mostly rectangular, area around the origin
 125 in the ambiguity plane. This resembles an approach taken to achieve high-resolution
 126 time-frequency distributions [80], [81], as we design the mask to pass auto-terms, and
 127 reduce cross-terms.

128 As an illustrative example of this approach, let us consider a sinusoidally-modulated
 129 signal with additive white Gaussian noise. For illustrative purposes, the time-frequency
 130 representations in Figure 1 are of size 60×60 points. Here, we consider a very small
 131 rectangular mask of size 7×7 points in the ambiguity domain, which represents just
 132 over one percent of the total number of samples. Now, let us consider the time-frequency
 133 representations of the signal. Figure 1(a) depicts the signal in the ambiguity domain
 134 which is observed as a domain of observations. The Wigner distribution is considered as
 135 a standard time-frequency distribution that can be derived from the ambiguity function in
 136 Figure 1(a) and it is the most appropriate to the considered signal type. This standard
 137 form of the time-frequency distribution is used only for the comparison purpose and
 138 it is calculated assuming the full set of samples from the ambiguity domain is available,
 139 Figure 1(b). Lastly, the compressive sensing based sparse time-frequency representation is
 140 presented in Figure 1(c). Unlike the standard time-frequency representation that requires
 141 full set of samples, the sparse representation is calculated from a very limited number
 142 of available samples. Despite this fact, we may observe that compared to the standard

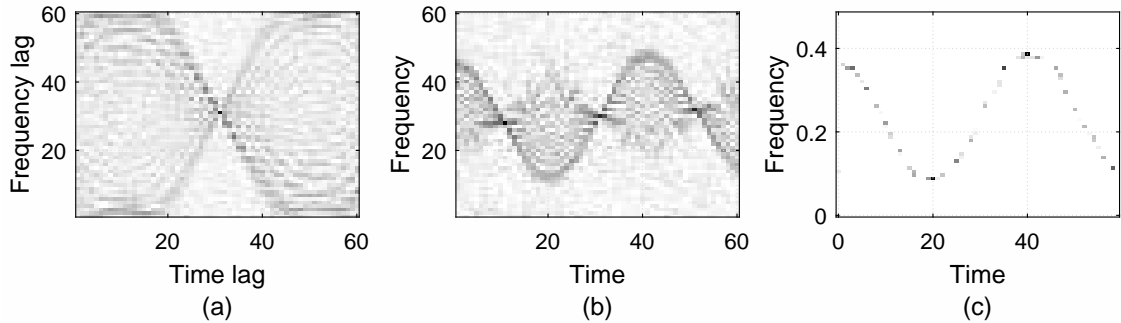


Figure 1: Representations of a sinusoidally-modulated signal in the time-frequency domain using: (a) the Wigner distributions, (b) the ambiguity function, (c) the resulting sparse time-frequency representation.

143 distribution (Figure 1(b)) the sparse representation achieved using compressive sensing
 144 approach offered a number of distinct advantages. First, it reduced the noise influence
 145 on the time-frequency representation, that is, it almost removed it completely from the
 146 distribution. Second, a number of non-zero terms in the sparse representation is about
 147 50, which represents slightly over one percent of the total number of points in the time-
 148 frequency domain. Hence, by compressively sensing the ambiguity representation of the
 149 signal, not only did we manage to compress the signal representation, but we also de-
 150 noised it.

151 An inherent issue with this approach is one requires the representation of a signal in
 152 the ambiguity domain. Hence, any hardware implementation of this approach is quite
 153 complex. Furthermore, this approach is applicable only to quadratic signal represen-
 154 tations, which limits our further signal manipulations (e.g., obtaining its time domain
 155 samples).

156 3.2. Compressive sensing based on time-frequency dictionary and matching pursuit

157 A more widely adopted approach is to utilize time-frequency dictionaries and obtain
 158 sparse signal representations using eqns. (2) and (3). Needless to say, this approach has
 159 very high computational costs which hindered its applications for many years. However,
 160 matching pursuit [82] or its variations (e.g., [83]) are very useful to avoid computational
 161 burdens associated with traditional compressive sensing approaches. Here, it is impor-
 162 tant to mention that a wide selection of time-frequency dictionaries exists, such as Gabor
 163 frames, curvelet frames, wavelet frames, overcomplete Fourier dictionaries or any combi-
 164 nations of these dictionaries [70], [84], [85], [86], [87], [88], [89], [90], [91].

Compressive sensing based implementation of a typical matching pursuit approach starts with an initial approximation of the signal, $\hat{x}^{(0)}(m) = 0$, and the residual, $R^{(0)}(m) = x(m)$. Here m represent the M time indices that are uniformly or non-uniformly distributed, that is, M time indices compressively acquired. At each subsequent stage, the matching pursuit algorithm identifies a dictionary atom with the strongest contribution to the residual and adds it to the current approximation:

$$\hat{x}^{(k)}(m) = \hat{x}^{(k-1)}(m) + \alpha_k \phi_k(m) \quad (11)$$

$$R^{(k)}(m) = x(m) - \hat{x}^{(k)}(m) \quad (12)$$

165 where $\alpha_k = \langle R^{(k-1)}(m), \phi_k(m) \rangle / \|\phi_k(m)\|^2$. The process continues till the norm of the
 166 residual $R^{(k)}(m)$ does not exceed required margin of error $\varepsilon > 0$: $\|R^{(k)}(m)\| \leq \varepsilon$ [82], or
 167 a number of bases, $\mathbf{n}_{\mathfrak{B}}$, needed for signal approximation should satisfy $\mathbf{n}_{\mathfrak{B}} \leq \mathcal{K}$. Lastly,
 168 an approximation of a compressively sampled signal is obtained using L bases as

$$x(n) = \sum_{l=1}^L \langle x(m), \phi_l(m) \rangle \phi_l(n) + R^{(L)}(n) \quad (13)$$

169 where ϕ_l are L bases from the dictionary with the strongest contributions. L bases used in
 170 the signal approximation are obtained regardless of the implemented stopping criterion.

171 The approach based on time-frequency dictionaries is suitable for any post-processing
 172 of compressively sampled signals. For example, we can easily obtain any time-frequency
 173 representation of a signal using this L -bases based approximation:

$$\mathcal{TF}\{x(n)\} = \sum_{l=1}^L \langle x(m), \phi_l(m) \rangle \mathcal{TF}\{\phi_l(n)\} \quad (14)$$

174 where $\mathcal{TF}\{\}$ is a time-frequency operator (e.g., the S-transform or short-time Fourier
 175 transform) [1], [92].

176 As mentioned in the previous paragraphs, M samples can be acquired in uniform
 177 or nonuniform manners and the exact time values are needed to acquire proper values
 178 of the time-frequency dictionary. Nevertheless, many real-life conditions may prevent
 179 us from acquiring such exact times, and there is a need to estimate the sampling time
 180 instances. This is achievable via annihilating filters contributions [38], [93], [94], which
 181 rely on determining the roots of an autoregressive filter in order to estimate the sampling
 182 instances.

183 3.2.1. A case study of a time-frequency dictionary for compressive sensing: Modulated
 184 discrete prolate spheroidal sequences

185 Discrete prolate spheroidal sequences were proposed by Slepian in 1978 [95]. For
 186 N samples and a normalized half-bandwidth value, W , a discrete prolate spheroidal
 187 sequence, $v_k(n, N, W)$, is defined as the real solution of [95]:

$$\sum_{m=0}^{N-1} \frac{\sin[2\pi W(n-m)]}{\pi(n-m)} v_k(m, N, W) = \lambda_k(N, W) v_k(n, N, W) \quad k = 0, 1, \dots, N-1 \quad (15)$$

188 with $0 < W < 0.5$, and $\lambda_k(N, W)$ being non-zero eigenvalues of (15). The amplitude of
 189 these eigenvalues can be also approximated for fixed k and large N as

$$1 - \lambda_k(N, W) \sim \frac{\sqrt{\pi}}{k!} 2^{\frac{14k+9}{4}} \alpha^{\frac{2k+1}{4}} [2 - \alpha]^{-(k+0.5)} N^{k+0.5} e^{-\gamma N} \quad (16)$$

190 where $\alpha = 1 - \cos(2\pi W)$ and $\gamma = \log \left[1 + \frac{2\sqrt{\alpha}}{\sqrt{2-\alpha}} \right]$. It can be shown that the first $2NW$
 191 eigenvalues are very close to 1 while the rest rapidly decays to zero [95]. These eigenvalues
 192 are also the eigenvalues of an $N \times N$ matrix $C(m, n)$ defined as [95]:

$$C(m, n) = \frac{\sin[2\pi W(n-m)]}{\pi(n-m)} \quad m, n = 0, 1, \dots, N-1. \quad (17)$$

193 By time-limiting a discrete prolate spheroidal sequence, $v_k(n, N, W)$, we can obtain an
 194 eigenvector of $C(m, n)$. The discrete prolate spheroidal sequences are doubly orthogonal,
 195 that is, they are orthogonal on the infinite set $\{-\infty, \dots, \infty\}$ and orthonormal on the finite
 196 set $\{0, 1, \dots, N-1\}$.

197 In recent years, discrete prolate spheroidal sequences were used to obtain sparse signal
 198 representations especially in the cases when these sequences and an analyzed signal are
 199 in the same frequency band [96], [97]. Nevertheless, when the sequences and the signal
 200 are not aligned in the frequency domain, a larger number of discrete prolate spheroidal
 201 sequences is needed to obtain an accurate approximation and resulting approximations
 202 are often not sparse. To avoid this issue with discrete prolate spheroidal sequences,
 203 modulated discrete prolate spheroidal sequences were proposed in [96], which are defined
 204 as:

$$M_k(N, W, \omega_m; n) = \exp(j\omega_m n) v_k(N, W; n) \quad (18)$$

205 where $\omega_m = 2\pi f_m$ is a modulating frequency. Modulated discrete prolate spheroidal
 206 sequences are also doubly orthogonal, have most of properties of original discrete prolate

207 spheroidal sequences and are bandlimited to the frequency band $[-W + \omega_m : W + \omega_m]$
 208 [96].

Choosing a proper modulation frequency ω_m requires some a priori knowledge, or a guess. The simplest case is when a signal is confined to a known band $[\omega_1; \omega_2]$, then the modulating frequency, ω_m , and the bandwidth of the modulated discrete prolate spheroidal sequences are given by

$$\omega_m = \frac{\omega_1 + \omega_2}{2} \quad (19)$$

$$W = \left| \frac{\omega_2 - \omega_1}{2} \right| \quad (20)$$

209 as long as both satisfy:

$$|\omega_m| + W < \frac{1}{2}. \quad (21)$$

210 Nevertheless, the exact frequency band is not known in many practical applications. In
 211 general, we will only have details about a relatively wide frequency band. To account
 212 for many different possibilities, we proposed to construct a time-frequency dictionary
 213 containing bases which reflect various bandwidth scenarios [96]. This approach was used
 214 in a number of recent compressive sensing contributions [98], [92], [99], [100].

215 A sample case, depicted in Figure 2(a), involves a signal consisting of four basis func-
 216 tions from a 25-band dictionary based on modulated discrete prolate spheroidal functions
 217 with the normalized half-bandwidth equal to $W = 0.495$ and $N = 256$. For both uniform
 218 and non-uniform sampling, only 42 samples were needed to accurately recover the signal
 219 (less than 17% of the total number of samples) and its spectrograms based on regular
 220 and irregular sample times as shown in 2(c) and (d). A greater percentage of samples
 221 was required for this case in comparison to the first case as the second case is recovered
 222 almost exactly.

223 3.3. Compressive sensing in the time-frequency domain using short-time Fourier trans- 224 form sparsity

225 Many of the signals appearing in real applications have a sparse representation in the
 226 Fourier transform domain, but also in the short-time Fourier transform domain [101],
 227 [102]. However, when the signal is affected by the noise, the number of non-zero compo-
 228 nents significantly increases thus ruining the sparsity, as shown in Figure 3(a) (its sorted

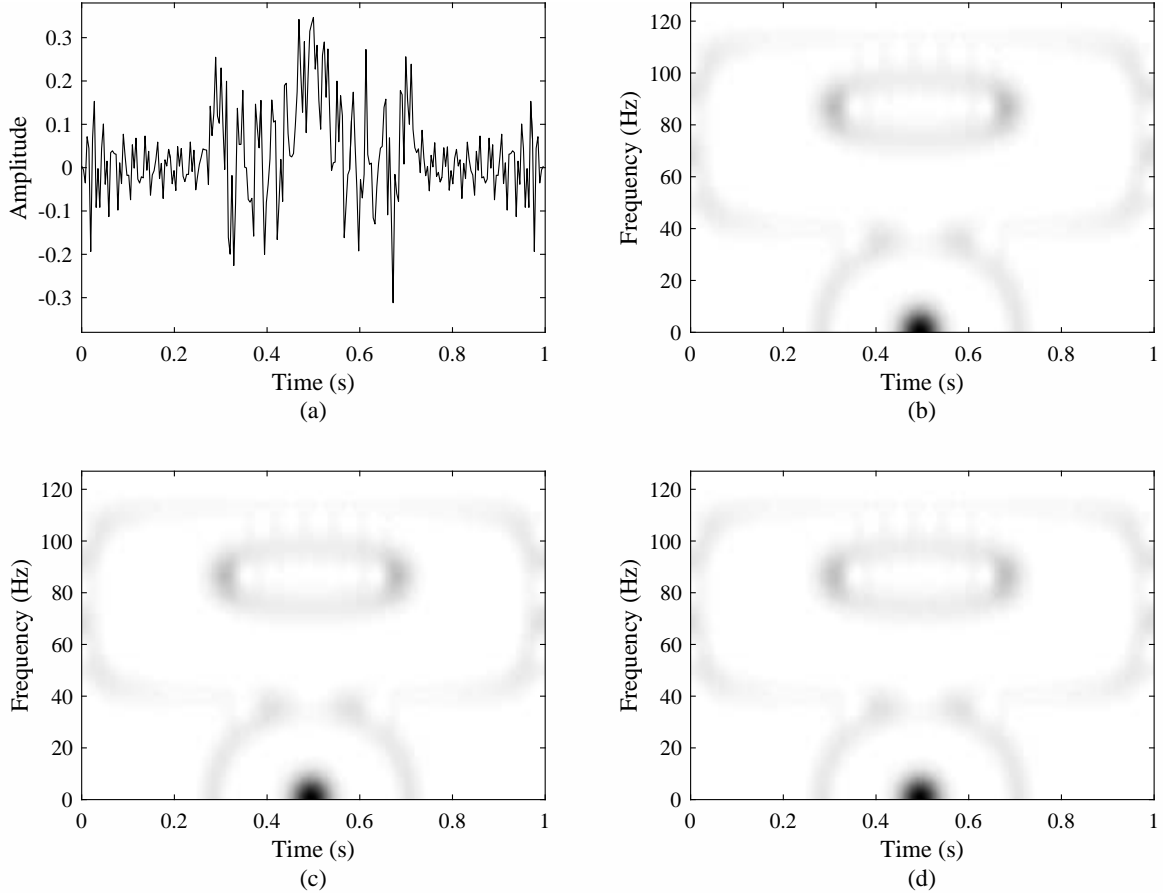


Figure 2: The time domain representation of the consider signal is shown in (a). Spectrograms of: (b) the original signal; (c) the signal based on equal distance samples; (d) the signal based on irregular samples.

229 values are shown in Figure 3(b)). By applying the L-estimation over columns of the short-
 230 time Fourier transform matrix, we may discard most of the unwanted coefficients from
 231 the short-time Fourier transform domain [103], [32]. However, many useful coefficients
 232 are also discarded in this process and we need to recover them using the compressive
 233 sensing approach. In the matrix form the short-time Fourier transform vector calculated
 234 at the time instant n using a rectangular window of size M can be defined as follow:

$$\begin{bmatrix} STFT(n, 0) \\ STFT(n, 1) \\ \vdots \\ STFT(n, M-1) \end{bmatrix} = \begin{bmatrix} \Psi(0, 0) & \dots & \Psi(0, M-1) \\ \Psi(1, 0) & \dots & \Psi(1, M-1) \\ \vdots & \dots & \vdots \\ \Psi(M-1, 0) & \dots & \Psi(M-1, M-1) \end{bmatrix} \begin{bmatrix} x(n) \\ x(n+1) \\ \vdots \\ x(n+M-1) \end{bmatrix} \quad (22)$$

235 or in a more compact form:

$$\mathbf{STFT}_M(n) = \Psi_M \mathbf{x}_M(n) \quad (23)$$

236 where Ψ_M is the discrete Fourier transform matrix of size $M \times M$:

$$\Psi(m, k) = \exp\left(-\frac{2\pi km}{M}\right) \quad m = 0, 1, \dots, M-1, k = 0, 1, \dots, M-1 \quad (24)$$

237 The index M denotes the size of corresponding vectors. For the sake of simplicity, let
 238 us assume the non-overlapping windows, meaning that the short-time Fourier transform
 239 is calculated for time instants n taken with the step $M : \{0, M, 2M, \dots, N - M\}$. The
 240 short-time Fourier transform calculation results in a set of short-time Fourier transform
 241 vectors: $\mathbf{STFT}_M(0), \mathbf{STFT}_M(M), \dots, \mathbf{STFT}_M(N - M)$. Therefore, the STFT for all
 242 considered time instants $n \in \{0, M, 2M, \dots, N - M\}$ is defined as follows [32]:

$$\begin{bmatrix} \mathbf{STFT}_M(0) \\ \mathbf{STFT}_M(M) \\ \vdots \\ \mathbf{STFT}_M(N - M) \end{bmatrix} = \begin{bmatrix} \Psi_M & \dots & 0_M \\ 0_M & \dots & 0_M \\ \vdots & \dots & \vdots \\ 0_M & \dots & \Psi_M \end{bmatrix} \begin{bmatrix} \mathbf{x}_M(0) \\ \mathbf{x}_M(M) \\ \vdots \\ \mathbf{x}_M(N - M) \end{bmatrix} \quad (25)$$

243 or equivalently: $STFT = \Theta \mathbf{x}$. The signal vector \mathbf{x} consists of N samples and can be
 244 expressed using a sparse vector \mathbf{X} of DFT coefficients:

$$\mathbf{x} = \Psi_N^{-1} \mathbf{X} \quad (26)$$

245 where Ψ_N^{-1} is the N -point inverse Fourier transform. Hence, the relationship between
 246 the short-time Fourier transform and discrete Fourier transform vectors can be written
 247 as follows:

$$\mathbf{STFT} = (\Theta \Psi_N^{-1}) \mathbf{X} = \mathbf{A} \mathbf{X}. \quad (27)$$

248 Now, let assume that the short-time Fourier transform is subject to L-estimation based
 249 filtering. After sorting the values of \mathbf{STFT} and discarding a certain percent of the
 250 highest and the lowest components, we are left with missing data in the short-time Fourier
 251 transform domain. On the positions of discarded components, the zero values remain
 252 (Figure 3(c)). Hence, a compressive sensing problem can be observed in the short-time
 253 Fourier transform domain:

$$\mathbf{y} = \mathbf{A}_{cs} \mathbf{X}. \quad (28)$$

254 where

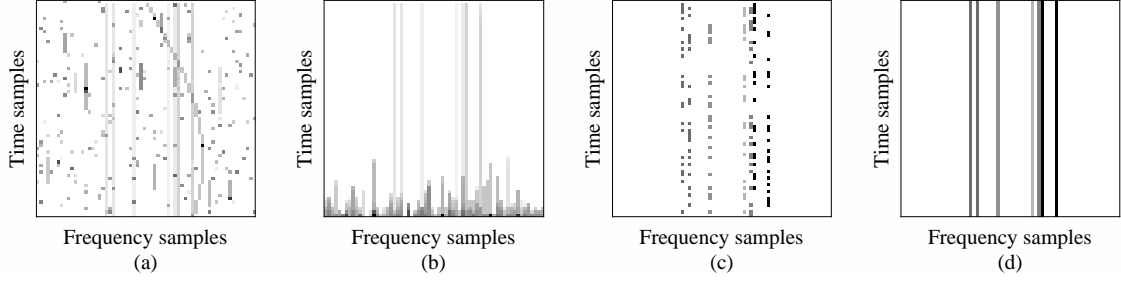


Figure 3: Compressive sensing and short-time Fourier transform: (a) noisy short-time Fourier transform; (b) sorted values of the noisy short-time Fourier transform; (c) available samples in the short-time Fourier transform after L-estimation; (d) reconstructed stationary components.

- 255 • \mathbf{y} is a vector of N_a available values from **STFT** (i.e., nonzero values);
- 256 • \mathbf{X} is a sparse discrete Fourier transform vector;
- 257 • \mathbf{A}_{cs} is obtained from $(\Theta\Psi_N^{-1})$ after removing the rows on the positions of missing
- 258 samples in **STFT**.

259 In order to reconstruct **STFT**, the minimization problem is observed in the form:

$$\min\|\mathbf{X}\|_1 \text{ s.t. } \mathbf{y} = \mathbf{A}_{cs}\mathbf{X}. \quad (29)$$

260 The reconstructed stationary components in the short-time Fourier transform domain are
 261 shown in Figure 3(d).

262 The amplitudes of the reconstructed components in the DFT domain corresponds
 263 to the original signal components: [2, 2, 1.5, 1, 1.7, 3.5, 3.5]. The proposed method is
 264 compared with the results produced by an ideal case of notch filter (its inverse form),
 265 where we need to assume that all signal frequencies are known. The ideal notch filter
 266 response will pick all values along the considered frequencies, meaning that will pick
 267 also the noise producing wrong amplitudes of certain signal components as follows. The
 268 recovered amplitudes of components are as follows: [2, 2, 1.5, 1.14, 2.17, 3.6, 3.76] as
 269 shown in Figure 4.

270 Finally, let us consider a real-world radar signal. The radar signal consist of five
 271 rigid body components (stationary components) and three corner reflectors rotating at
 272 60 RPM (nonstationary components). The stationary and non-stationary components
 273 intersects in both time and frequency dimensions. The short-time Fourier transformation

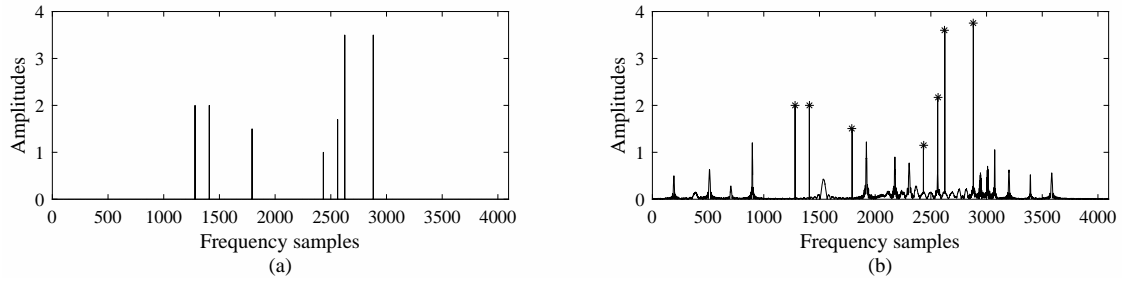


Figure 4: Comparing time-frequency based compressive sensing approaches and a notch filter: (a) reconstructed frequency components obtained using the proposed approach; (b) noisy components that would be selected by an ideal notch filter are marked by '*'.

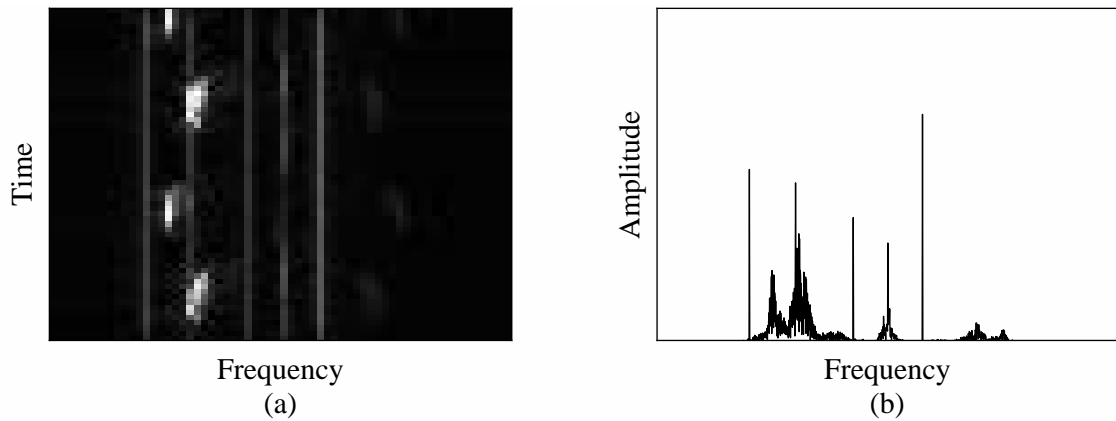


Figure 5: A sample radar signal: (a) the short-time Fourier transform of the observed signal; (b) the corresponding Fourier transform.

274 of the observed signal is shown in Figure 5(a), while the Fourier transform of the signal
 275 is shown in Figure 5(b).

276 The goal is to separate the micro-Doppler and rigid body components. As previously
 277 described, the short-time Fourier transform is calculated using non-overlapping windows
 278 (Figure 6(a)). The values in the short-time Fourier transform matrix are then sorted and
 279 50% of lowest values are discarded. Namely, the micro-Doppler components appears to be
 280 smaller valued than the rigid body components in the sorted time-frequency signal repre-
 281 sentation because of their shorter duration. The remaining short-time Fourier transform
 282 values are shown in Figure 6(b) and represent the compressive sensing measurements
 283 that are subject to the compressive sensing reconstruction procedure. The reconstructed
 284 stationary rigid body components are shown in Figure 6(c), while the remaining micro-
 285 Doppler components are shown in Figure 6(d).

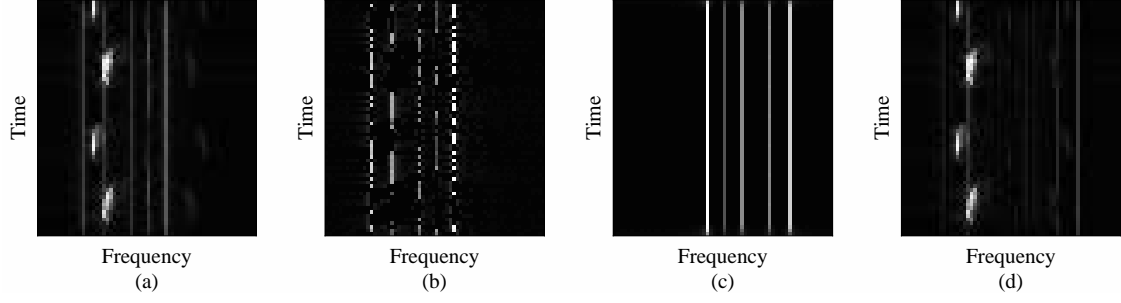


Figure 6: Compressive sensing and the short-time Fourier transform: (a) the short-time Fourier transform of the signal; (b) available samples in the short-time Fourier transform after L-estimation; (c) extracted rigid body components; (d) extracted micro-Doppler components.

286 3.4. Compressive sensing of signals based on the polynomial Fourier transform

287 The sparse representation of polynomial phase signals can be achieved by applying
 288 the polynomial Fourier transform [104]. The polynomial Fourier transform of signals $s(n)$
 289 can be defined as follows:

$$X(k_1, \dots, k_L) = \sum_{n=0}^{N-1} s(n) \exp \left\{ -j \frac{2\pi}{N} \left(\frac{n^2 k_2}{2} + \dots + \frac{n^L k_L}{L!} \right) - j \frac{2\pi}{N} n k_1 \right\} \quad (30)$$

290 where the polynomial coefficients are assumed to be bounded integers. If $s(n)$ is a mono-
 291 component polynomial phase signal of the form:

$$s(n) = A \exp \left\{ j \frac{2\pi}{N} \left(n \varphi_1 \frac{n^2 \varphi_2}{2} + \dots + \frac{n^L \varphi_L}{L!} \right) \right\} \quad (31)$$

292 and if a set of polynomial Fourier transform coefficients (k_2, k_3, \dots, k_L) match the signal
 293 phase parameters $(\varphi_2, \varphi_3, \dots, \varphi_L)$:

$$k_2 = \varphi_2, k_3 = \varphi_3, \dots, k_L = \varphi_L \quad (32)$$

294 then we will obtain the sinusoid in the polynomial Fourier transform domain at the
 295 position $k_1 = \varphi_1$. Otherwise, the polynomial Fourier transform of $s(n)$ is not sparse. In
 296 that sense, the polynomial Fourier transform transform can be observed as the discrete
 297 Fourier transform of $s(n)$ demodulated by the exponential term $d(n)$:

$$X(k_1, \dots, k_L) = \sum_{n=0}^{N-1} s(n) d(n) \exp \left\{ -j \frac{2\pi}{N} n k_1 \right\} \quad (33)$$

298 where

$$d(n) = \exp \left\{ -j \frac{2\pi}{N} \left(\frac{n^2 k_2}{2} + \dots + \frac{n^L k_L}{L!} \right) \right\} \quad (34)$$

299 The situation becomes more complex when $s(n)$ is a K -component polynomial phase
 300 signal:

$$s_K(n) = \sum_{i=1}^K A_i \exp \left\{ j \frac{2\pi}{N} \left(na_{1i} + \frac{n^2 a_{2i}}{2} + \dots + \frac{n^L a_{Li}}{L!} \right) \right\}. \quad (35)$$

301 The coefficients of demodulation term $d(n)$ should be then chosen to correspond to one
 302 of the components:

$$k_2 = \varphi_{i2}, k_3 = \varphi_{i3}, \dots, k_L = \varphi_{iL}. \quad (36)$$

303 As a result, the i th signal component is demodulated and becomes a sinusoid in the
 304 polynomial Fourier transform domain [105]. The polynomial Fourier transform represen-
 305 tation is not strictly sparse as in the case of a single polynomial phase signal, but the
 306 i th component will be dominant in the polynomial Fourier transform spectrum. In that
 307 sense, we might say that if $k_2 = \varphi_{i2}, k_3 = \varphi_{i3}, \dots, k_L = \varphi_{iL}$ is satisfied, then the poly-
 308 nomial Fourier transform is compressible with the dominant i th component. Note that the
 309 sparsity (compressibility) in the polynomial Fourier transform domain is observed with
 310 respect to the single demodulated component. Thus, we need to change the values of
 311 polynomial Fourier transform coefficients k_2, k_3, k_L within a certain range $[k_{min}, k_{max}]$ un-
 312 til we obtain a dominant component in the polynomial Fourier transform domain, which
 313 means that we revealed one of the K signal components: $k_2 = \varphi_{i2}, k_3 = \varphi_{i3}, \dots, k_L = \varphi_{iL}$,
 314 $i \in [1, K]$.

315 In the compressive sensing context, the signal vector \mathbf{s} is randomly undersampled
 316 having only $N_a \ll N$ available samples. It means that the demodulation vector \mathbf{d} should
 317 be also calculated only for N_a available instants. Now, the measurement vector \mathbf{y} can be
 318 defined as follows [105]:

$$\mathbf{y} = \mathbf{s}(n_a) \mathbf{d}(n_a) = \mathbf{x}(n_a) \quad (37)$$

319 where n_a denotes available sample positions.

320 The vector form of the polynomial Fourier transform definition given by eqn. (33) is
 321 given by:

$$\mathbf{X} = \Psi_N \mathbf{x} \quad (38)$$

322 where Ψ_N^N is a $N \times N$ discrete Fourier transform matrix. From eqns. (37) and (38), we
 323 may write:

$$\mathbf{y} = \Psi_{N_a}^{-1} \mathbf{X} \quad (39)$$

Algorithm 1 Calculate compressive sensing based polynomial Fourier transform

Require: $n_a > 0$

```

for  $k_j = k_{min} : \text{step} : k_{max}, j = 2, \dots, L$  do
   $\mathbf{y} = \mathbf{s}(n_a)\mathbf{d}(n_a)$ 
   $\mathbf{X} = \Psi_{N_a}\mathbf{y}$ 
  if  $k_2 = \varphi_{i2}, k_3 = \varphi_{i3}, \dots, k_L = \varphi_{iL} \Leftrightarrow$  there is a dominant sinusoid  $\mathbf{X}_i$  then
     $k_{1i} = \arg \max(\mathbf{X})$ 
    Save  $\mathbf{k}_i = (k_1, k_2, \dots, k_L) = (\varphi_{1i}, \varphi_{2i}, \dots, \varphi_{Li})$ 
  end if
end for

```

324 where $\Psi_{N_a}^{-1}$ is the partial random inverse Fourier matrix of size $N_a \times N$ obtained by
 325 omitting rows from inverse discrete Fourier transform matrix $\Psi_{N_a}^{-1}$ that correspond to
 326 the unavailable samples. If the demodulation term is chosen such that $k_2 = \varphi_{i2}, k_3 =$
 327 $\varphi_{i3}, \dots, k_L = \varphi_{iL}$ then \mathbf{X} can be observed as a demodulated version of the i th signal
 328 component \mathbf{X}_i , having the dominant i th component in the spectrum with the support
 329 k_{1i} . Other components in spectrum are much lower than \mathbf{X}_i and could be observed as
 330 noise. The minimization problem can be written in the form:

$$\min \|\mathbf{X}_i\|_1 \text{ subject to } \|\mathbf{y}\Psi_{N_a}^{-1}\mathbf{X}\|_2 < \xi. \quad (40)$$

331 The procedure can be described in the form of pseudo code as shown in Algorithm 1.
 332 Hence, as a result of this phase we have identified the sets of signal phase parameters:
 333 $\mathbf{k}_i = (k_1, k_2, \dots, k_L) = (\varphi_{1i}, \varphi_{2i}, \dots, \varphi_{Li})$.

334 Next, we need to recover the exact components amplitudes. Denote the set of available
 335 signal samples positions by $\mathbf{n}_a = (n_1, n_2, \dots, n_{N_a})$. In order to calculate the exact amplitudes
 336 A_1, A_2, \dots, A_K of K signal components, we observe the set of equations in the form:

$$\begin{bmatrix} s(n_1) \\ s(n_2) \\ \vdots \\ s(n_{N_a}) \end{bmatrix} = \begin{bmatrix} \Phi(1, 1) & \dots & \Phi(1, K) \\ \Phi(2, 1) & \dots & \Phi(2, K) \\ \vdots & \dots & \vdots \\ \Phi(N_a, 1) & \dots & \Phi(N_a, K) \end{bmatrix} \begin{bmatrix} A_1 \\ A_2 \\ \vdots \\ A_K \end{bmatrix} \quad (41)$$

337 where

$$\Phi(j, i) = \exp \left\{ j \frac{2\pi}{N} (n_j k_{1i} + \dots + n_j^L k_{Li}) \right\} \quad j = 1, \dots, N_a; i = 1, \dots, K. \quad (42)$$

338 In other words we have another system of equations given by:

$$\mathbf{s}(n_a) = \mathbf{\Phi}\alpha \quad (43)$$

339 where $\alpha = [A_1, \dots, A_K]^T$ contains the desired K signal amplitudes. The rows of $\mathbf{\Phi}$ cor-
 340 respond to positions of measurements n_1, n_2, \dots, n_{N_a} , and columns correspond to the K
 341 components with phase parameters $(k_1, k_2, \dots, k_L) = (\varphi_{1i}, \varphi_{2i}, \dots, \varphi_{Li})$, for $i = 1, \dots, K$.
 342 The solution of the observed problem can be obtained in the least square sense as:

$$\alpha = (\mathbf{\Phi}^* \mathbf{\Phi})^{-1} \mathbf{\Phi}^* \sim(n_a) \quad (44)$$

343 Let us consider a polynomial phase signal in the form that consists of three chirp com-
 344 ponents:

$$\begin{aligned} s(t) &= s_1(t) + s_2(t) + s_3(t) \\ &= \exp(-j\pi\varphi_{21}t^2 + j\pi\varphi_{11}t) + \exp(-j\pi\varphi_{22}t^2 + j\pi\varphi_{12}t) + \exp(-j\pi\varphi_{23}t^2 + j\pi\varphi_{13}t) \\ &= \exp(-j\pi 8Tt^2 + j\pi 16Tt) + \exp(-j\pi 32Tt^2 + j\pi 16Tt) + \exp(-j\pi 8Tt^2 + j\pi 16Tt) \end{aligned}$$

345 where the signal parameters are given as: $t = [-1/2, 1/2)$ with step $\Delta t = 1/1024$, $T = 32$,
 346 and the total signal length is 1024 samples. Observe that there are three chirp components
 347 with the rates: $\varphi_{21} = 8T$, $\varphi_{22} = 32T$, $\varphi_{23} = 8T$. The demodulation term is given in the
 348 form $d(t) = \exp(j2\pi k_2 T t^2)$. We need to search for parameter k_2 . Thus, we change the
 349 values of parameter k_2 within a predefined range to match components one after the
 350 other. The discrete Fourier transform spectrum of full length signal before applying the
 351 demodulation term (as a part of the polynomial Fourier transform) is shown in Figure
 352 7(a). When $k_2 = -8T$, the first component is detected and it becomes dominant in the
 353 spectrum (Figure 7(b)). The same situation appears when $k_2 = 32T$ (Figure 7(c)) and
 354 $k_2 = 8T$ (Figure 7(d)).

355 We may observe that the polynomial Fourier transform with an appropriate demodu-
 356 lation term $d(t)$ can be considered as compressible for the dominant component matched
 357 by the demodulation term. As such, it is amenable for compressive sensing reconstruction.

358 Next, we consider a small number of randomly selected available samples, i.e., 128 out
 359 of 1024 are available (12.5% of the total signal length). The missing samples within $s(t)$
 360 are considered as zero values, and then the demodulation term is applied iteratively for

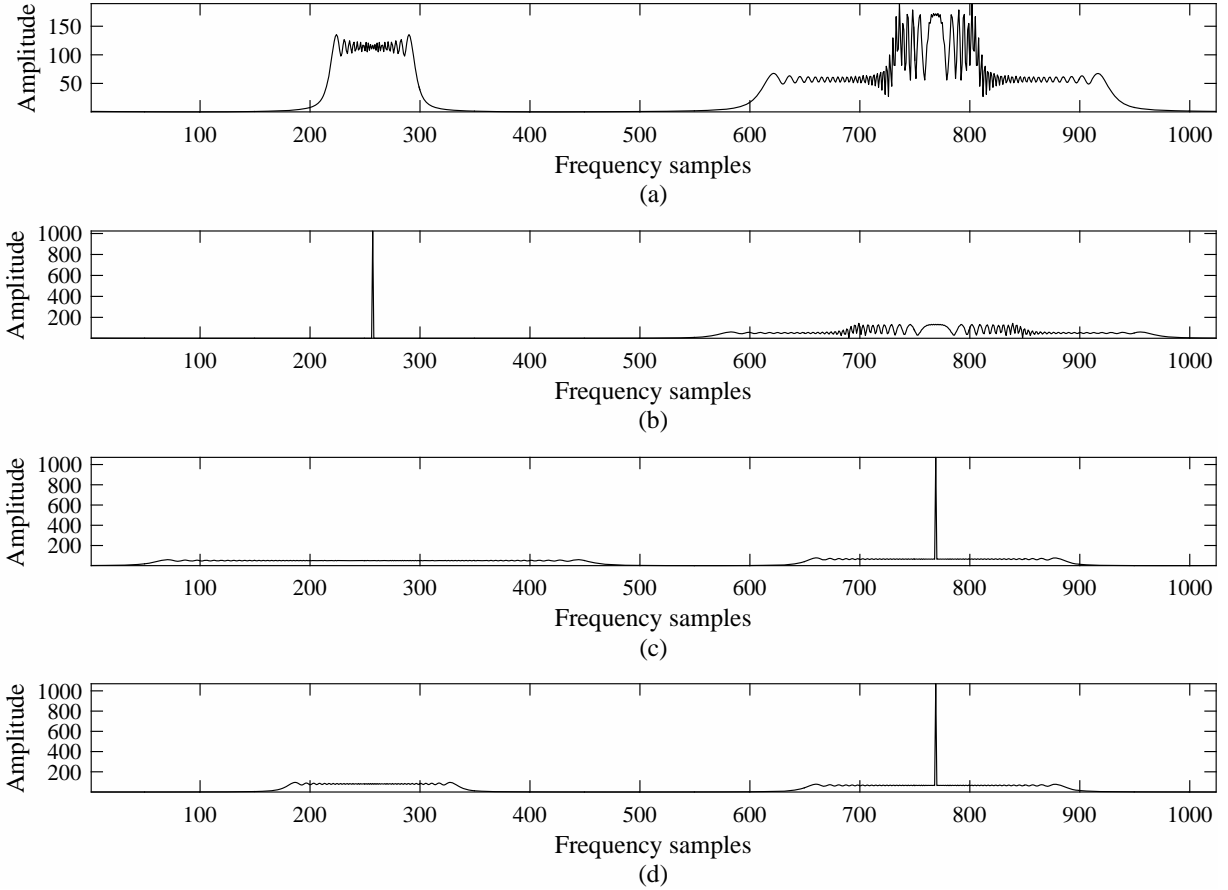


Figure 7: The effects of demodulation on the discrete Fourier transform spectrum: (a) the discrete Fourier transform of $s(t)$ before demodulation; (b) demodulation with $k_2 = -8T$; (c) demodulation with $k_2 = 32T$; (d) demodulation with $k_2 = 8T$.

361 a range of values k_2 . The results for the PFT when k_2 matches $\varphi_{21} = -8T$, $\varphi_{22} = 32T$
362 and $\varphi_{23} = 8T$ are given in Figures 8(a)-(c). Note that noise appears as a consequence
363 of missing samples that are set to zero value in order to calculate the initial polynomial
364 Fourier transform. However, the demodulated components are prominent in the spectrum
365 (Figure 8). For the illustration, Figure 9 depicts the initial polynomial Fourier transform
366 when k_2 does not match any of φ_{21} , φ_{22} and φ_{23} . The spectrum is noisy with no dominant
367 components revealed.

368 The compressive sensing reconstruction method needs to determine the support of
369 components revealed after the appropriate demodulation as shown in Figure 8. In the
370 same time, it should ignore the cases with inappropriate k_2 . The simplest solution can
371 be achieved using a threshold derived for the single iteration compressive sensing recon-
372 struction algorithm, proposed in [106]. When the threshold (horizontal red line in Fig.

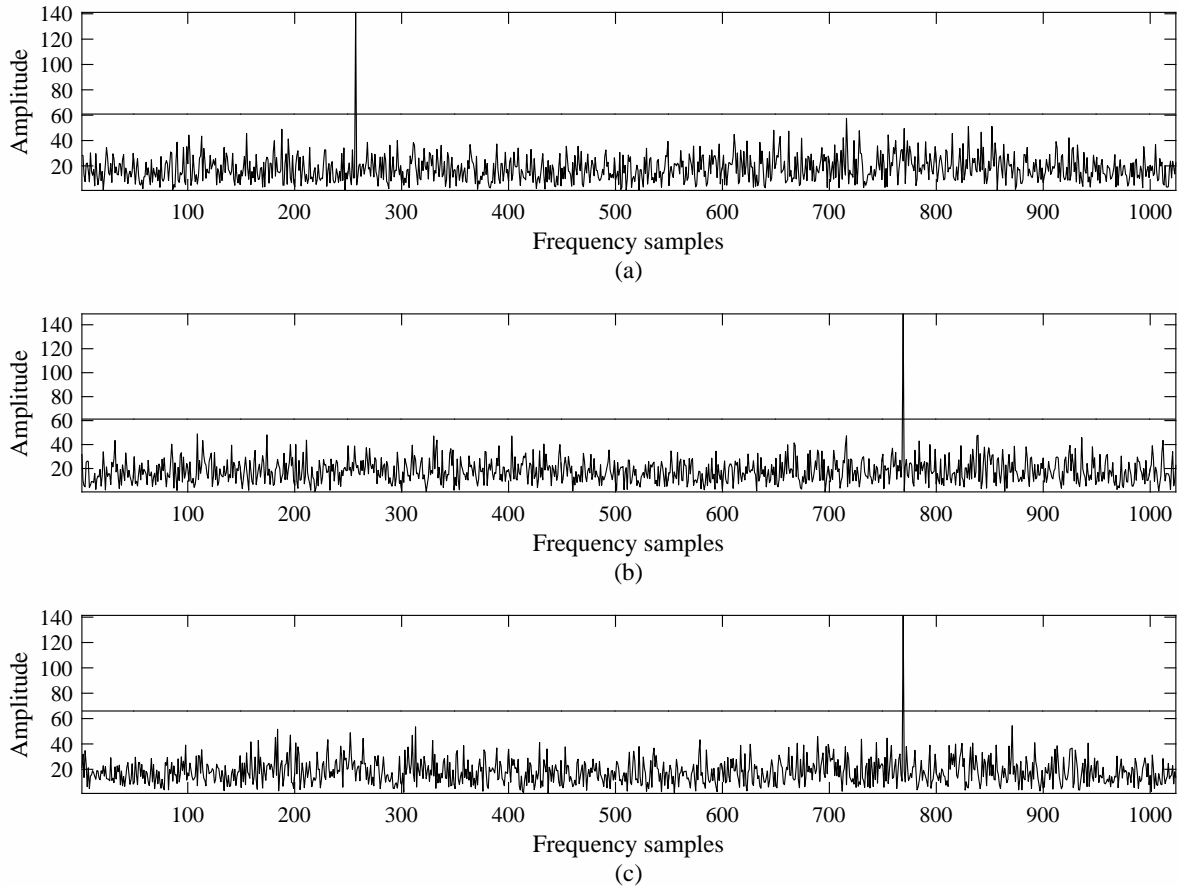


Figure 8: The polynomial Fourier transform for the compressive sensing case: (a) demodulation with $\varphi_{21} = -8T$; (b) demodulation with $\varphi_{22} = 32T$; (c) demodulation with $\varphi_{23} = 8T$.

373 3) is applied on the spectrum after demodulation with appropriate k_2 (k_2 matches either
374 $\varphi_{21} = -8T$, $\varphi_{22} = 32T$ and $\varphi_{23} = 8T$), a support of demodulated component is returned
375 as a result: $\varphi_{11} = -8T$, $\varphi_{12} = -16T$ and $\varphi_{13} = 16T$. Otherwise, when the threshold is
376 applied to the spectrum after demodulation with inappropriate (wrong k_2), the method
377 returns no support (Figure 9).

378 4. Compressive sensing based time-frequency representations

379 Most of time-frequency distributions can be observed as the Fourier transforms of
380 the local autocorrelation functions. In order to produce highly localized energy distribu-
381 tions, the autocorrelation functions must locally approximate a sinusoidal signal at each
382 time sample. The overall instantaneous frequency characteristics are obtained based on
383 the individual sinusoidal frequencies from different shifted signal windows [107], [108],

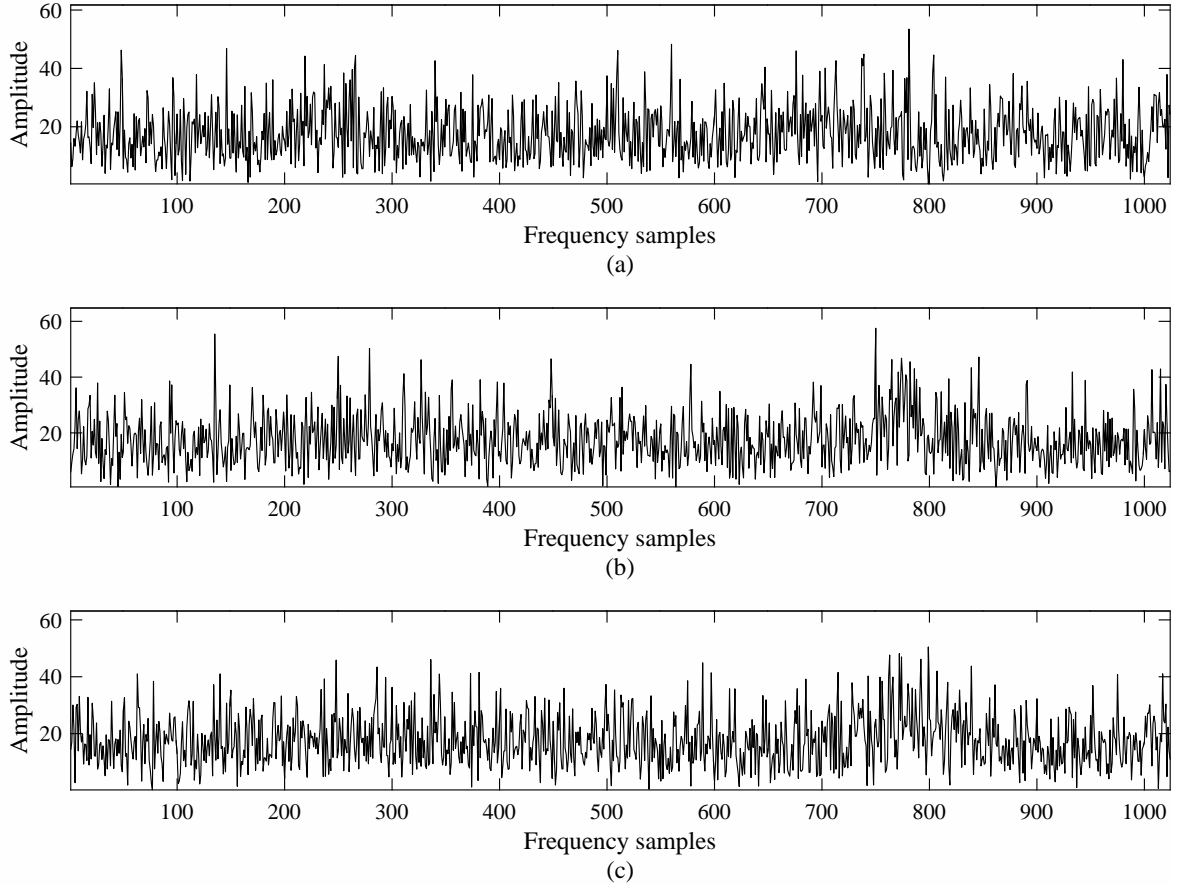


Figure 9: Compressive sensing of the polynomial Fourier transform with an incorrect demodulation term: (a) demodulation with $k_2 = 18T$; (b) demodulation with $k_2 = 12T$; (c) demodulation with $k_2 = 16T$

384 [109], [110]. In the context of compressive sensing, we observe the case when a signal
385 is represented by a small set of random samples. Consequently, only a small percent
386 of total autocorrelation function samples are considered as available for time-frequency
387 distribution calculations and instantaneous frequency estimations. The standard form
388 of time-frequency distributions calculated from coarsely under-sampled autocorrelation
389 functions would be seriously degraded by noise, with amplitudes of components being
390 much below their true values. As a solution, we can consider compressive sensing based
391 time-frequency representations obtained by applying the compressive sensing reconstruc-
392 tion algorithm to autocorrelation functions, in lieu of the Fourier transform, to achieve
393 an ideal time-frequency signal representations [111], [112].

394 We can start with a definition of time-frequency distributions defined as the Fourier

395 transform of a higher order local autocorrelation function:

$$TFD(t, f) = \int_{-\infty}^{+\infty} R(t, \tau) e^{-j2\pi\tau} d\tau. \quad (45)$$

396 The general form of the local autocorrelation function can be defined as follows:

$$R(t, \tau) = \prod_{i=1}^{P/2} x^{b_i}(t + a_i\tau) x^{*b_i}(t - a_i\tau) \quad (46)$$

397 where P is an even number representing the order of a distribution, while the coefficients
 398 a_i and b_i depend on a particular time-frequency distribution. Without loss of generality,
 399 the rectangular window function is assumed. For instance,

- 400 1. The Wigner distribution is obtained when $P = 2$ and $a_1 = 1/2$, and $b_1 = 1$.
- 401 2. The L-Wigner distribution is obtained when $P = 2$, $a_1 = 1/(2L)$, and $b_1 = L$ as it
 402 yields $R(t, \tau) = x^L(t + \frac{\tau}{2L}) x^{*L}(t - \frac{\tau}{2L})$.
- 403 3. For $P = 4$ and $a_1 = 0.675$, $b_1 = 2$, $a_2 = -0.85$, $b_2 = 1$, the auto-correlation function
 404 in given by $R(t, \tau) = x^2(t + 0.675\tau) x^{*2}(t - 0.675\tau) x(t - 0.85\tau) x^*(t + 0.85\tau)$, which
 405 leads to the polynomial distribution.

406 Now, assume that only a small number of M random samples from $R(t, \tau)$ are available
 407 in each windowed part where $M \ll N$ holds (N is the total number of samples within
 408 the window). For the sake of simplicity we may write the autocorrelation function in the
 409 form:

$$R(t, \tau) = x_1 x_2 \dots x_p = \prod_{i=1}^P x_i \quad (47)$$

410 and

$$R(t, \tau) = \begin{cases} R(t, \tau_{n_m}) & m = 1, \dots, M \\ 0 & \text{otherwise} \end{cases} \quad (48)$$

411 where the discrete signal terms are denoted by vectors x_i , while τ_{n_m} for $m = 1, \dots, M$ are
 412 random positions of available samples in one lag-window. Hence, we have:

$$\|R(t, \tau)\|_{l_0} = \left\| \prod_{i=1}^P x_i \right\|_{l_0} = M. \quad (49)$$

413 The standard TFD calculated on the basis of $R(t, \tau)$ with missing samples, would be
 414 affected by the noise due to the missing samples. Namely, the missing samples needs to

415 be considered as zero values in $R(t, \tau)$ which will produce noise in the time-frequency
 416 domain. Hence, we consider the possibility to apply the concept of CS reconstruction
 417 in order to provide a noise-free time-frequency representation. If we observe the vec-
 418 tor of autocorrelation samples for a single time instant t_j denoted as $R(t, \tau)$, then the
 419 optimization problem can be defined as follows:

$$\min \|\mathbf{X}(t_j, \tau)\|_{l_1} \text{ subject to } R(t_j, \tau) = \mathbf{A}\mathbf{X}(t_j, f) \quad (50)$$

420 where for the observed t_j , $\mathbf{X}(t_j, f)$ represents a sparse vector belonging to an ideal time-
 421 frequency representation at the time instant t_j . The matrix \mathbf{A} is the Fourier transform
 422 based compressive sensing matrix. The minimization problem can be solved using some of
 423 the known compressive sensing reconstruction algorithms, such as the orthogonal match-
 424 ing pursuit.

425 Let us consider an illustrative example in the form:

$$x_1(t) = \exp(j160\pi t^3 - j190\pi t) \quad (51)$$

426 The polynomial distribution of the fourth order is considered for a time-frequency rep-
 427 resentation of the observed signal. The amount of available samples \mathbf{x}_1 is 35% of the
 428 total number of window samples ($N = 128$ samples). The standard polynomial distribu-
 429 tion calculated with zero values on the positions of missing samples in auto-correlation
 430 function is shown in Figure 10(a). In order to provide the compressive sensing based time-
 431 frequency representation, the orthogonal matching pursuit is applied to each windowed
 432 signal part in order to recover sparse spectrum corresponding to each particular time
 433 instant. It means that in the case of the considered monocomponent signal, a single fre-
 434 quency component is obtained for each time instant, resulting in an ideal time-frequency
 435 representation as shown in Figure 10(b).

436 Similarly, let us consider a signal with a fast varying instantaneous frequency given in
 437 the form:

$$x_2(t) = \exp(j6 \sin(2.4\pi t) + j3 \cos(1.5\pi t) - j20\pi t^2) \quad (52)$$

438 As a suitable time-frequency distribution, the complex-time distribution is usually con-
 439 sidered for fast varying instantaneous frequency estimations, since it provides significant

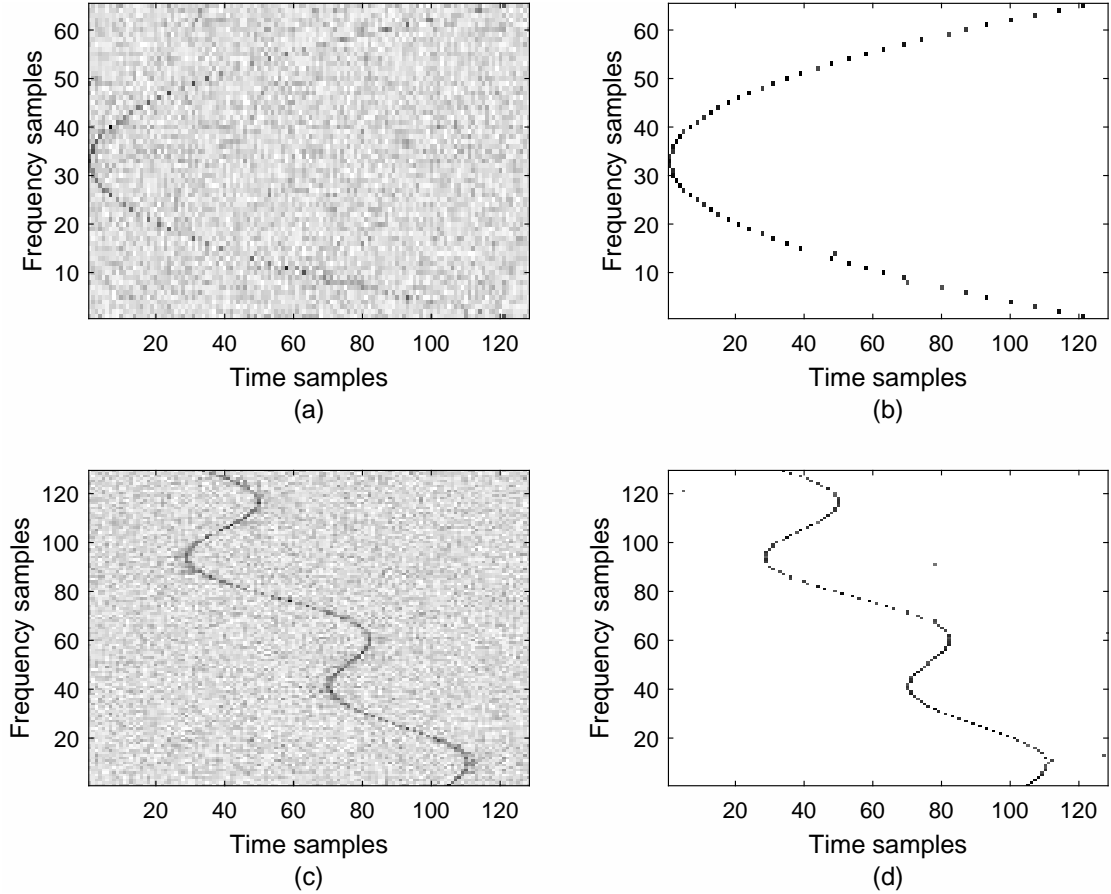


Figure 10: Comparison between the traditional time-frequency distributions and their compressive sensing based equivalents: (a) the traditional polynomial distribution $x_1(t)$, (b) a compressive sensing based polynomial distribution of $x_1(t)$ (c) the traditional complex-time distribution of $x_2(t)$, (d) a compressive sensing variant of the complex-time distribution of $x_2(t)$.

440 concentration improvements with respect to the quadratic but also polynomial distribu-
 441 tions [113], [114]. A commonly used complex-lag distribution is defined for the autocor-
 442 relation function in the form:

$$R(t, \tau) = x\left(t + \frac{\tau}{4}\right) x^{-1}\left(t - \frac{\tau}{4}\right) x^{-j}\left(t + j\frac{\tau}{4}\right) x^j\left(t - j\frac{\tau}{4}\right) \quad (53)$$

443 Let us assume that for \mathbf{x}_2 , there is approximately 40% of available samples. The stan-
 444 dard form of the complex-time distributions and its improved compressive sensing version
 445 are provided in Figures 10(c) and 10(d). The compressive sensing based complex-time
 446 distribution provides almost an ideal representation for the instantaneous frequency esti-
 447 mation. Compared to the standard form, the compressive sensing based form is noiseless
 448 and highly compressible providing a set of enhanced peaks along the instantaneous fre-

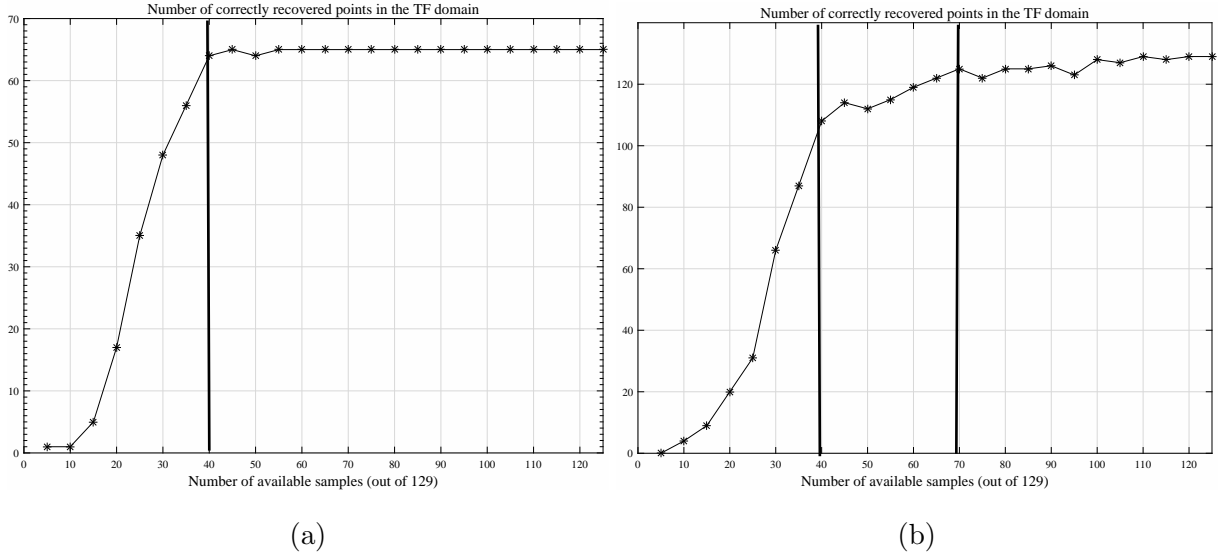


Figure 11: Estimated numbers of points to accurately estimate instantaneous frequency with (a) the polynomial distribution; (b) the complex-time distribution.

449 quency, while the other values in the tim-frequency plane are zeros.

450 Next, we estimated the required number of available samples that can provide an
 451 accurate instantaneous frequency representation after the reconstruction in the time-
 452 frequency domain. The results are shown in Figures 11a and 11b for the polynomial
 453 distribution and the complex-time distribution, respectively. The assumed signal length
 454 is 129 samples. In the case of the polynomial distribution, a high level of precision
 455 (100% of points are exactly reconstructed) is achieved with 30% of available samples
 456 (40 samples out of 129). For the complex-time distribution, we can observe that the
 457 acceptable precision is achieved even with 30% of available samples (app. 40 samples out
 458 of 129), while in the case when the amount of available samples is 55% or more (app. 70
 459 samples or more), the accurate estimation is achieved.

460 While these illustrative examples depict that the major advantage of these approaches
 461 is the fact that we can obtain very accurate representations of non-stationary signals even
 462 a small number of samples, it needs to be pointed out that these compressive sensing based
 463 time-frequency approaches are computationally more expensive than traditional time-
 464 frequency approaches. The increased computational complexity is due to the optimization
 465 procedure implemented to recover missing samples.

466 5. Conclusions and future directions

467 In this review paper, we summarized recent advances regarding compressive sensing
468 and time-frequency analysis. All these recent contributions demonstrate that compres-
469 sive sensing provided a framework for sparse time-frequency processing of non-stationary
470 signals. Based on the current contributions, we anticipate the following future directions:

- 471 • There is a great need to develop hardware solutions for all these signal processing
472 schemes consider in this paper. Hardware developments are severely lagging the
473 algorithmic development, which currently leaves many questions unanswered when
474 it comes to practical applicability of these algorithms.
- 475 • Compressive sensing based time-frequency representations address a major issue
476 associated with traditional time-frequency representations, that is, the ability to
477 obtain a time-frequency representation of a signal using only a small number of ran-
478 dom samples. However, the major disadvantage of these approaches is that they are
479 much more computationally expansive than traditional time-frequency approaches.
480 Hence, future research directions include the development of computationally in-
481 expensive compressive sensing based time-frequency representations, that have the
482 computational cost of the same order as traditional time-frequency methods.
- 483 • Adaptations of these new algorithms in many different areas is still an open ques-
484 tions. While there are applications that have highly redundant information and
485 can tolerate errors (e.g., communication systems) for which compressive sensing
486 provides excellent results, there are many more that require compressive sensing to
487 provide perfect reconstruction every time (e.g., most of medical diagnostic applica-
488 tions). Hence, the time-frequency based compressive sensing approaches have the
489 largest value in these applications requiring very high accuracies, as typical com-
490 pressive sensing approaches based on random basis dictionaries are not suitable.

491 In conclusion, this paper provides a concise summary of the work in compressive sensing
492 for sparse time-frequency processing. While the framework provides very powerful tools
493 to process sparse non-stationary signals, we strongly believe it is still in its early stages,
494 and it is expected that further research and applications of the existing schemes will grow

495 in the near future. In our companion paper [115], we describe MATLAB functions used
496 to generate figures presented in this manuscript.

497 **Acknowledgments**

498 The work of E. Sejdić was partially funded by the Eunice Kennedy Shriver National
499 Institute of Child Health & Human Development of the National Institutes of Health
500 under Award Number R01HD074819. The content is solely the responsibility of E. Sejdić
501 and does not necessarily represent the official views of the National Institutes of Health.

502 **References**

- 503 [1] E. Sejdić, I. Djurović, and J. Jiang, “Time-frequency feature representation using
504 energy concentration: An overview of recent advances,” *Digital Signal Processing*,
505 vol. 19, no. 1, pp. 153–183, Jan. 2009.
- 506 [2] A. N. Akansu and R. A. Haddad, *Multiresolution Signal Decomposition: Trans-*
507 *forms, Subbands, and Wavelets*. San Diego: Academic Press, 2001.
- 508 [3] M. Akay, Ed., *Time-Frequency and Wavelets in Biomedical Signal Processing*. Pis-
509 cataway, NJ: IEEE Press, 1998.
- 510 [4] R. E. Challis and R. I. Kitney, “Biomedical signal processing (in four parts) - part
511 1: Time-domain methods,” *Medical and Biological Engineering and Computing*,
512 vol. 28, no. 6, pp. 509–524, Nov. 1990.
- 513 [5] I. Orović, M. Orlandić, S. Stanković, and Z. Uskoković, “A virtual instrument
514 for time-frequency analysis of signals with highly nonstationary instantaneous fre-
515 quency,” *IEEE Transactions on Instrumentation and Measurement*, vol. 60, no. 3,
516 pp. 791–803, March 2011.
- 517 [6] B. Boashash, Ed., *Time-Frequency Signal Analysis and Processing: A Comprehen-*
518 *sive Reference*, 2nd ed. Amsterdam: Elsevier, 2016.
- 519 [7] K. Gröchenig, *Foundations of Time-Frequency Analysis*. Boston: Birkhäuser, 2001.

- 520 [8] S. Stanković, I. Orović, and E. Sejdić, *Multimedia Signals and Systems: Basic and*
521 *Advanced Algorithms for Signal Processing*, 2nd ed. New York, NY: Springer US,
522 2016.
- 523 [9] A. Cohen and J. Kovačević, “Wavelets: The mathematical background,” *Proceed-*
524 *ings of the IEEE*, vol. 84, no. 4, pp. 514–522, Apr. 1996.
- 525 [10] S. Stanković, I. Orović, and A. Krylov, “Video frames reconstruction based on
526 time-frequency analysis and Hermite projection method,” *EURASIP Journal on*
527 *Advances in Signal Processing*, vol. 2010, no. 1, p. 970105, 2010.
- 528 [11] F. Hlawatsch and G. Boudreaux-Bartels, “Linear and quadratic time-frequency
529 signal representations,” *IEEE Signal Processing Magazine*, vol. 9, no. 2, pp. 21–67,
530 Apr. 1992.
- 531 [12] X. Li, G. Bi, S. Stankovic, and A. M. Zoubir, “Local polynomial fourier transform:
532 A review on recent developments and applications,” *Signal Processing*, vol. 91, no. 6,
533 pp. 1370–1393, 2011.
- 534 [13] S. Stanković and I. Orović, “Time-frequency rate distributions with complex-lag
535 argument,” *Electronics Letters*, vol. 46, no. 13, pp. 950–952, June 2010.
- 536 [14] P. J. Kootsookos and B. C. L. B. Boashash, “A unified approach to the STFT,
537 TFDs, and instantaneous frequency,” *IEEE Transactions on Signal Processing*,
538 vol. 40, no. 8, pp. 1971–1982, Aug. 1992.
- 539 [15] S. Stanković, I. Orović, and V. Sucic, “Averaged multiple l-spectrogram for analysis
540 of noisy nonstationary signals,” *Signal Processing*, vol. 92, no. 12, pp. 3068–3074,
541 2012.
- 542 [16] S. Blanco, R. Q. Quiroga, O. A. Rosso, and S. Kochen, “Time-frequency analysis
543 of electroencephalogram series,” *Physical Review E*, vol. 51, no. 3, pp. 2624–2631,
544 Mar. 1995.
- 545 [17] C. Li, C. Zheng, and C. Tai, “Detection of ECG characteristic points using wavelet

- 546 transforms,” *IEEE Transactions on Biomedical Engineering*, vol. 42, no. 1, pp.
547 21–28, Jan. 1995.
- 548 [18] S. Blanco, R. Q. Quiroga, O. A. Rosso, and S. Kochen, “Time-frequency analysis
549 of electroencephalogram series II. Gabor and wavelet transforms,” *Physical Review*
550 *E*, vol. 54, no. 6, pp. 6661–6672, Dec. 1996.
- 551 [19] P. M. Bentley, P. M. Grant, and J. T. E. McDonnell, “Time-frequency and
552 time-scale techniques for the classification of native and bioprosthetic heart valve
553 sounds,” *IEEE Transactions on Biomedical Engineering*, vol. 45, no. 1, pp. 125–128,
554 Jan. 1998.
- 555 [20] M. Stridh, L. Sörnmo, C. J. Meurling, and S. B. Olsson, “Sequential characteri-
556 zation of atrial tachyarrhythmias based on ECG time-frequency analysis,” *IEEE*
557 *Transactions on Biomedical Engineering*, vol. 51, no. 1, pp. 100–114, Jan. 2004.
- 558 [21] I. Orović, S. Stanković, T. Chau, C. M. Steele, and E. Sejdić, “Time-frequency anal-
559 ysis and Hermite projection method applied to swallowing accelerometry signals,”
560 *EURASIP Journal on Advances in Signal Processing*, pp. 323 125–1–7., 2010.
- 561 [22] E. Sejdić, K. A. Lowry, J. Bellanca, M. S. Redfern, and J. S. Brach, “A comprehen-
562 sive assessment of gait accelerometry signals in time, frequency and time-frequency
563 domains,” *IEEE Transactions on Neural Systems and Rehabilitation Engineering*,
564 vol. 22, no. 3, pp. 603–612, May 2014.
- 565 [23] H. Bleton, S. Perera, and E. Sejdić, “Cognitive tasks and cerebral blood flow
566 through anterior cerebral arteries: a study via functional transcranial doppler ul-
567 trasound recordings,” *BMC Medical Imaging*, vol. 16, no. 1, p. 22, 2016.
- 568 [24] A. G. Rehorn, E. Sejdić, and J. Jiang, “Fault diagnosis in machine tools using
569 selective regional correlation,” *Mechanical Systems and Signal Processing*, vol. 20,
570 no. 5, pp. 1221–1238, Jul. 2006.
- 571 [25] H. Oehlmann, D. Brie, M. Tomczak, and A. Richard, “A method for analysing gear-
572 box faults using time-frequency representations,” *Mechanical Systems and Signal*
573 *Processing*, vol. 11, no. 4, pp. 529–545, Nov. 1997.

- 574 [26] W. J. Staszewski, K. Worden, and G. R. Tomlinson, "Time-frequency analysis in
575 gearbox fault detection using the Wigner-Ville distribution and pattern recogni-
576 tion," *Mechanical Systems and Signal Processing*, vol. 11, no. 5, pp. 673–692, Sep.
577 1997.
- 578 [27] J. Lin and L. Qu, "Feature extraction based on Morlet wavelet and its application
579 for mechanical fault diagnosis," *Journal of Sound and Vibration*, vol. 234, no. 1,
580 pp. 135–148, Jun. 2000.
- 581 [28] G. Tzanetakis and P. Cook, "Musical genre classification of audio signals," *IEEE*
582 *Transactions on Speech and Audio Processing*, vol. 10, no. 5, pp. 293–302, Jul. 2002.
- 583 [29] K. Umaphy, S. Krishnan, and S. Jimaa, "Multigroup classification of audio signals
584 using time-frequency parameters," *IEEE Transactions on Multimedia*, vol. 7, no. 2,
585 pp. 308–315, Apr. 2005.
- 586 [30] B. Boashash and P. O'Shea, "A methodology for detection and classification of
587 some underwater acoustic signals using time-frequency analysis techniques," *IEEE*
588 *Transactions on Acoustics, Speech, and Signal Processing*, vol. 38, no. 11, pp. 1829–
589 1841, Nov. 1990.
- 590 [31] LJ. Stanković, T. Thayaparan, and M. Daković, "Signal decomposition by using
591 the S-method with application to the analysis of HF radar signals in sea-clutter,"
592 *IEEE Transactions on Signal Processing*, vol. 54, no. 11, pp. 4332–4342, Nov. 2006.
- 593 [32] L. Stanković, S. Stanković, T. Thayaparan, M. Daković, and I. Orović, "Separation
594 and reconstruction of the rigid body and micro-Doppler signal in ISAR Part I -
595 theory," *IET Radar, Sonar Navigation*, vol. 9, no. 9, pp. 1147–1154, 2015.
- 596 [33] —, "Separation and reconstruction of the rigid body and micro-Doppler signal
597 in ISAR Part ii - statistical analysis," *IET Radar, Sonar Navigation*, vol. 9, no. 9,
598 pp. 1155–1161, 2015.
- 599 [34] L. Stanković, I. Orović, S. Stanković, and M. Amin, "Compressive sensing based
600 separation of nonstationary and stationary signals overlapping in time-frequency,"
601 *IEEE Transactions on Signal Processing*, vol. 61, no. 18, pp. 4562–4572, Sept 2013.

- 602 [35] Y. Sun and J. Li, “Time-frequency analysis for plastic landmine detection via
603 forward-looking ground penetrating radar,” *IEE Proceedings - Radar, Sonar and*
604 *Navigation*, vol. 150, no. 4, pp. 253–261, Aug. 2003.
- 605 [36] Y. Zhang, M. Amin, and G. Frazer, “High-resolution time-frequency distributions
606 for manoeuvring target detection in over-the-horizon radars,” *IEE Proceedings -*
607 *Radar, Sonar and Navigation*, vol. 150, no. 4, pp. 299–304, Aug. 2003.
- 608 [37] L. Brechet, M.-F. Lucas, C. Doncarli, and D. Farina, “Compression of biomedical
609 signals with mother wavelet optimization and best-basis wavelet packet selection,”
610 *IEEE Transactions on Biomedical Engineering*, vol. 54, no. 12, pp. 2186–2192, Dec.
611 2007.
- 612 [38] M. Vetterli, P. Marziliano, and T. Blu, “Sampling signals with finite rate of innova-
613 tion,” *IEEE Transactions on Signal Processing*, vol. 50, no. 6, pp. 1417–1428, Jun.
614 2002.
- 615 [39] D. L. Donoho, “Compressed sensing,” *IEEE Transactions on Information Theory*,
616 vol. 52, no. 4, pp. 1289–1306, Apr. 2006.
- 617 [40] W. Dai and O. Milenković, “Subspace pursuit for compressive sensing signal recon-
618 struction,” *IEEE Transaction on Information Theory*, vol. 55, no. 5, pp. 2230–2249,
619 May 2009.
- 620 [41] I. Orović, A. Draganić, and S. Stanković, “Sparse time-frequency representation for
621 signals with fast varying instantaneous frequency,” *IET Radar, Sonar Navigation*,
622 vol. 9, no. 9, pp. 1260–1267, 2015.
- 623 [42] K.-K. Poh and P. Marziliano, “Compressive sampling of EEG signals with finite
624 rate of innovation,” *EURASIP Journal on Advances in Signal Processing*, vol. 2010,
625 pp. 183 105–1–12, 2010.
- 626 [43] A. M. Abdulghani, A. J. Casson, and E. Rodriguez-Villegas, “Compressive sens-
627 ing scalp EEG signals: implementations and practical performance,” *Medical &*
628 *Biological Engineering & Computing*, vol. 50, no. 11, pp. 1137–1145, 2012.

- 629 [44] M. Lustig, D. L. Donoho, J. M. Santos, and J. M. Pauly, “Compressed sensing
630 mri,” *IEEE Signal Processing Magazine*, vol. 25, no. 2, pp. 72–82, March 2008.
- 631 [45] J. H. Ender, “On compressive sensing applied to radar,” *Signal Processing*, vol. 90,
632 no. 5, pp. 1402–1414, 2010.
- 633 [46] B. Han, F. Wu, and D. Wu, “Image representation by compressive sensing for visual
634 sensor networks,” *Journal of Visual Communication and Image Representation*,
635 vol. 21, no. 4, pp. 325–333, 2010.
- 636 [47] W. U. Bajwa, J. Haupt, A. M. Sayeed, and R. Nowak, “Compressed channel sensing:
637 A new approach to estimating sparse multipath channels,” *Proceedings of the IEEE*,
638 vol. 98, no. 6, pp. 1058–1076, June 2010.
- 639 [48] Y. Rivenson, A. Stern, and B. Javidi, “Overview of compressive sensing techniques
640 applied in holography,” *Applied Optics*, vol. 52, no. 1, pp. A423–A432, Jan 2013.
- 641 [49] L. Stanković, S. Stanković, and M. Amin, “Missing samples analysis in signals for
642 applications to l-estimation and compressive sensing,” *Signal Processing*, vol. 94,
643 pp. 401–408, 2014.
- 644 [50] D. Craven, B. McGinley, L. Kilmartin, M. Glavin, and E. Jones, “Compressed
645 sensing for bioelectric signals: A review,” *IEEE Journal of Biomedical and Health
646 Informatics*, vol. 19, no. 2, pp. 529–540, March 2015.
- 647 [51] S. Stanković, I. Orović, and M. Amin, “L-statistics based modification of reconstruc-
648 tion algorithms for compressive sensing in the presence of impulse noise,” *Signal
649 Processing*, vol. 93, no. 11, pp. 2927–2931, 2013.
- 650 [52] I. Orovic, V. Papic, C. Ioana, X. Li, and S. Stankovic, “Compressive sensing in
651 signal processing: Algorithms and transform domain formulations,” *Mathematical
652 Problems in Engineering*, 2016, article ID 7616393, 16 page.
- 653 [53] J. Bobin, J. L. Starck, and R. Ottensamer, “Compressed sensing in astronomy,”
654 *IEEE Journal of Selected Topics in Signal Processing*, vol. 2, no. 5, pp. 718–726,
655 Oct 2008.

- 656 [54] Y. Wiaux, L. Jacques, G. Puy, A. M. M. Scaife, and P. Vandergheynst, “Compressed
657 sensing imaging techniques for radio interferometry,” *Monthly Notices of the Royal*
658 *Astronomical Society*, vol. 395, no. 3, p. 1733, 2009.
- 659 [55] C. R. Berger, S. Zhou, J. C. Preisig, and P. Willett, “Sparse channel estimation
660 for multicarrier underwater acoustic communication: From subspace methods to
661 compressed sensing,” *IEEE Transactions on Signal Processing*, vol. 58, no. 3, pp.
662 1708–1721, March 2010.
- 663 [56] Y. Chi, L. L. Scharf, A. Pezeshki, and A. R. Calderbank, “Sensitivity to basis
664 mismatch in compressed sensing,” *IEEE Transactions on Signal Processing*, vol. 59,
665 no. 5, pp. 2182–2195, May 2011.
- 666 [57] M. F. Duarte and Y. C. Eldar, “Structured compressed sensing: From theory to
667 applications,” *IEEE Transactions on Signal Processing*, vol. 59, no. 9, pp. 4053–
668 4085, Sept 2011.
- 669 [58] S. Qaisar, R. M. Bilal, W. Iqbal, M. Naureen, and S. Lee, “Compressive sensing:
670 From theory to applications, a survey,” *Journal of Communications and Networks*,
671 vol. 15, no. 5, pp. 443–456, Oct 2013.
- 672 [59] G. Tang, B. N. Bhaskar, P. Shah, and B. Recht, “Compressed sensing off the grid,”
673 *IEEE Transactions on Information Theory*, vol. 59, no. 11, pp. 7465–7490, Nov
674 2013.
- 675 [60] R. Leary, Z. Saghi, P. A. Midgley, and D. J. Holland, “Compressed sensing electron
676 tomography,” *Ultramicroscopy*, vol. 131, pp. 70–91, 2013.
- 677 [61] A. Veeraraghavan, D. Reddy, and R. Raskar, “Coded strobing photography: Com-
678 pressive sensing of high speed periodic videos,” *IEEE Transactions on Pattern*
679 *Analysis and Machine Intelligence*, vol. 33, no. 4, pp. 671–686, April 2011.
- 680 [62] S. Ganguli and H. Sompolinsky, “Compressed sensing, sparsity, and dimensionality
681 in neuronal information processing and data analysis,” *Annual Review of Neuro-*
682 *science*, vol. 35, pp. 485–508, 2012.

- 683 [63] A. Massa, P. Rocca, and G. Oliveri, “Compressive sensing in electromagnetics - a
684 review,” *IEEE Antennas and Propagation Magazine*, vol. 57, no. 1, pp. 224–238,
685 Feb 2015.
- 686 [64] H. Rauhut, K. Schnass, and P. Vandergheynst, “Compressed sensing and redundant
687 dictionaries,” *IEEE Transactions on Information Theory*, vol. 54, no. 5, pp. 2210
688 –2219, May 2008.
- 689 [65] O. Teke, A. C. Gurbuz, and O. Arikan, “A robust compressive sensing based tech-
690 nique for reconstruction of sparse radar scenes,” *Digital Signal Processing*, vol. 27,
691 pp. 23–32, 2014.
- 692 [66] R. G. Baraniuk, “Compressive sensing,” *IEEE Signal Processing Magazine*, vol. 24,
693 no. 4, pp. 118–121, Jul. 2007.
- 694 [67] E. J. Candes and M. B. Wakin, “An introduction to compressive sampling,” *IEEE*
695 *Signal Processing Magazine*, vol. 25, no. 2, pp. 21–30, Mar. 2008.
- 696 [68] C. R. Berger, S. Zhou, J. C. Preisig, and P. Willett, “Sparse channel estimation
697 for multicarrier underwater acoustic communication: From subspace methods to
698 compressed sensing,” *IEEE Transactions on Signal Processing*, vol. 58, no. 3, pp.
699 1708–1721, March 2010.
- 700 [69] T. Strohmer, “Measure what should be measured: Progress and challenges in com-
701 pressive sensing,” *IEEE Signal Processing Letters*, vol. 19, no. 12, pp. 887–893, Dec
702 2012.
- 703 [70] E. J. Candes, Y. C. Eldar, D. Needell, and P. Randall, “Compressed sensing with
704 coherent and redundant dictionaries,” *Applied and Computational Harmonic Anal-*
705 *ysis*, vol. 31, no. 1, pp. 59–73, 2011.
- 706 [71] M. Elad, “Optimized projections for compressed sensing,” *IEEE Transactions on*
707 *Signal Processing*, vol. 55, no. 12, pp. 5695–5702, Dec 2007.
- 708 [72] L. C. Potter, E. Ertin, J. T. Parker, and M. Cetin, “Sparsity and compressed

- 709 sensing in radar imaging,” *Proceedings of the IEEE*, vol. 98, no. 6, pp. 1006–1020,
710 June 2010.
- 711 [73] B. Adcock, C. Hansen, C. Poon, and B. Roman, “Breaking the coherence barrier:
712 A new theory for compressed sensing,” *Forum of Mathematics, Sigma*, vol. 5, 2017.
- 713 [74] G. E. Pfander and H. Rauhut, “Sparsity in time-frequency representations,” *Journal*
714 *of Fourier Analysis and Applications*, vol. 16, no. 2, pp. 233–260, 2010.
- 715 [75] Y. Wang, J. Xiang, Q. Mo, and S. He, “Compressed sparse timefrequency
716 feature representation via compressive sensing and its applications in fault
717 diagnosis,” *Measurement*, vol. 68, pp. 70–81, 2015. [Online]. Available:
718 <http://www.sciencedirect.com/science/article/pii/S0263224115001049>
- 719 [76] M. G. Amin, B. Jokanovic, Y. D. Zhang, and F. Ahmad, “A sparsity-perspective
720 to quadratic timefrequency distributions,” *Digital Signal Processing*, vol. 46, pp.
721 175–190, 2015.
- 722 [77] G. Orchard, J. Zhang, Y. Suo, M. Dao, D. T. Nguyen, S. Chin, C. Posch, T. D. Tran,
723 and R. Etienne-Cummings, “Real time compressive sensing video reconstruction in
724 hardware,” *IEEE Journal on Emerging and Selected Topics in Circuits and Systems*,
725 vol. 2, no. 3, pp. 604–615, Sept 2012.
- 726 [78] P. Flandrin and P. Borgnat, “Time-frequency energy distributions meet compressed
727 sensing,” *IEEE Transactions on Signal Processing*, vol. 58, no. 6, pp. 2974–2982,
728 Jun. 2010.
- 729 [79] T. A. C. M. Claasen and W. F. G. Mecklenbrauker, “The Wigner distribution -
730 a tool for time frequency signal analysis: Part I Continuous time signals,” *Philips*
731 *Journal of Research*, vol. 35, no. 3, pp. 217–250, 1980.
- 732 [80] B. Boashash, G. Azemi, and J. M. O’Toole, “Time-frequency processing of nonsta-
733 tionary signals: Advanced TFD design to aid diagnosis with highlights from medical
734 applications,” *IEEE Signal Processing Magazine*, vol. 30, no. 6, pp. 108–119, Nov.
735 2013.

- 736 [81] B. Jokanovic and M. Amin, “Reduced interference sparse time-frequency distri-
737 butions for compressed observations,” *IEEE Transactions on Signal Processing*,
738 vol. 63, no. 24, pp. 6698–6709, Dec 2015.
- 739 [82] S. G. Mallat and Z. Zhang, “Matching pursuits with time-frequency dictionaries,”
740 *IEEE Transactions on Signal Processing*, vol. 41, no. 12, pp. 3397–3415, Dec. 1993.
- 741 [83] D. Needell and J. A. Tropp, “Cosamp: Iterative signal recovery from incomplete
742 and inaccurate samples,” *Applied and Computational Harmonic Analysis*, vol. 26,
743 no. 3, pp. 301–321, May 2009.
- 744 [84] L. Hu, Z. Shi, J. Zhou, and Q. Fu, “Compressed sensing of complex sinusoids: An
745 approach based on dictionary refinement,” *IEEE Transactions on Signal Processing*,
746 vol. 60, no. 7, pp. 3809–3822, July 2012.
- 747 [85] Y. Zhang, B. Dong, and Z. Lu, “ l_0 minimization of wavelet frame based image
748 restoration,” *Mathematics of Computation*, vol. 82, pp. 995–1015, 2013.
- 749 [86] T. Y. HOU and Z. SHI, “Adaptive data analysis via sparse time-frequency repre-
750 sentation,” *Advances in Adaptive Data Analysis*, vol. 03, no. 01n02, pp. 1–28, Apr.
751 2011.
- 752 [87] D. Angelosante, G. B. Giannakis, and N. D. Sidiropoulos, “Sparse parametric mod-
753 els for robust nonstationary signal analysis: Leveraging the power of sparse regres-
754 sion,” *IEEE Signal Processing Magazine*, vol. 30, no. 6, pp. 64–73, Nov. 2013.
- 755 [88] G. Taubock, F. Hlawatsch, D. Eiwen, and H. Rauhut, “Compressive estimation
756 of doubly selective channels in multicarrier systems: Leakage effects and sparsity-
757 enhancing processing,” *IEEE Journal of Selected Topics in Signal Processing*, vol. 4,
758 no. 2, pp. 255–271, April 2010.
- 759 [89] T. Y. Hou and Z. Shi, “Data-driven timefrequency analysis,” *Applied and Compu-
760 tational Harmonic Analysis*, vol. 35, no. 2, pp. 284–308, 2013.

- 761 [90] A. C. Gurbuz, V. Cevher, and J. H. McClellan, "Bearing estimation via spatial spar-
762 sity using compressive sensing," *IEEE Transactions on Aerospace and Electronic*
763 *Systems*, vol. 48, no. 2, pp. 1358–1369, APRIL 2012.
- 764 [91] A. Perelli, L. D. Marchi, L. Flamigni, A. Marzani, and G. Masetti, "Best basis
765 compressive sensing of guided waves in structural health monitoring," *Digital Signal*
766 *Processing*, vol. 42, pp. 35–42, 2015.
- 767 [92] E. Sejdić and L. F. Chaparro, "Time-frequency representations based on com-
768 pressive samples," in *Proc. of 21st European Signal Processing Conference (EU-*
769 *SIPCO'13)*, Marrakech, Morocco, Sep. 9–13, 2013, pp. 1 569 742 057–1–4.
- 770 [93] S. Senay, L. F. Chaparro, and L. Durak, "Reconstruction of nonuniformly sampled
771 time-limited signals using prolate spheroidal wave functions," *Signal Processing*,
772 vol. 89, no. 12, pp. 2585–2595, Dec. 2009.
- 773 [94] T. Blu, P.-L. Dragotti, M. Vetterli, P. Marziliano, and L. Coulot, "Sparse sampling
774 of signal innovations," *IEEE Signal Processing Magazine*, vol. 25, no. 2, pp. 31–40,
775 Mar. 2008.
- 776 [95] D. Slepian, "Prolate spheroidal wave functions, Fourier analysis, and uncertainty
777 - V: The discrete case," *The Bell System Technical Journal*, vol. 57, no. 5, pp.
778 1371–1430, May/Jun. 1978.
- 779 [96] E. Sejdić, M. Luccini, S. Primak, K. Baddour, and T. Willink, "Channel estimation
780 using DPSS based frames," in *IEEE International Conference on Acoustics, Speech*
781 *and Signal Processing (ICASSP 2008)*, Las Vegas, Nevada, USA, Mar./Apr. 31–4,
782 2008, pp. 2849–2852.
- 783 [97] T. Zemen and C. F. Mecklenbräuker, "Time-variant channel estimation using
784 discrete prolate spheroidal sequences," *IEEE Transactions on Signal Processing*,
785 vol. 53, no. 9, pp. 3597–3607, Sep. 2005.
- 786 [98] E. Sejdić, A. Can, L. F. Chaparro, C. M. Steele, and T. Chau, "Compressive sam-
787 pling of swallowing accelerometry signals using time-frequency dictionaries based on

- 788 modulated discrete prolate spheroidal sequences,” *EURASIP Journal on Advances*
789 *in Signal Processing*, vol. 2012, pp. 101–1–14, May 2012.
- 790 [99] J. Oh, S. Senay, and L. F. Chaparro, “Signal reconstruction from nonuniformly
791 spaced samples using evolutionary Slepian transform-based POCS,” *EURASIP*
792 *Journal on Advances in Signal Processing*, vol. 2010, pp. 367 317–1–12, 2010.
- 793 [100] E. Sejdić and L. F. Chaparro, “Recovering heart sounds from sparse samples,”
794 in *Proc. of 38th Annual Northeast Bioengineering Conference (NEBEC 2012)*,
795 Philadelphia, PA, USA, Mar. 16–18, 2012, pp. 107–108.
- 796 [101] V. C. Chen, F. Li, S. S. Ho, and H. Wechsler, “Micro-Doppler effect in radar:
797 phenomenon, model, and simulation study,” *IEEE Transactions on Aerospace and*
798 *Electronic Systems*, vol. 42, no. 1, pp. 2–21, Jan 2006.
- 799 [102] M. Martorella, “Novel approach for isar image cross-range scaling,” *IEEE Trans-*
800 *actions on Aerospace and Electronic Systems*, vol. 44, no. 1, pp. 281–294, January
801 2008.
- 802 [103] I. Djurović and L. Stanković, “Realization of robust filters in the frequency domain,”
803 *IEEE Signal Processing Letters*, vol. 9, no. 10, pp. 333–335, Oct 2002.
- 804 [104] V. Katkovnik, “A new form of the Fourier transform for time-varying frequency
805 estimation,” *Signal Processing*, vol. 47, no. 2, pp. 187–200, Nov. 1995.
- 806 [105] S. Stanković, I. Orović, and L. Stanković, “Polynomial Fourier domain as a domain
807 of signal sparsity,” *Signal Processing*, vol. 130, pp. 243–253, 2017.
- 808 [106] ———, “An automated signal reconstruction method based on analysis of compressive
809 sensed signals in noisy environment,” *Signal Processing*, vol. 104, pp. 43–50, 2014.
- 810 [107] B. Boashash, “Estimating and interpreting the instantaneous frequency of a signal
811 - part 1: Fundamentals,” *Proceedings of the IEEE*, vol. 80, no. 4, pp. 520–538, Apr.
812 1992.

- 813 [108] —, “Estimating and interpreting the instantaneous frequency of a signal - part 2:
814 Algorithms and applications,” *Proceedings of the IEEE*, vol. 80, no. 4, pp. 540–568,
815 Apr. 1992.
- 816 [109] B. Boashash, Ed., *Time-Frequency Signal Analysis and Processing: A Comprehensive Reference*. Amsterdam: Elsevier, 2003.
- 818 [110] J. Lerga and V. Sucic, “Nonlinear IF estimation based on the pseudo WVD adapted
819 using the improved sliding pairwise ICI rule,” *IEEE Signal Processing Letters*,
820 vol. 16, no. 11, pp. 953–956, Nov 2009.
- 821 [111] I. Orović, S. Stanković, and T. Thayaparan, “Time-frequency-based instantaneous
822 frequency estimation of sparse signals from incomplete set of samples,” *IET Signal*
823 *Processing*, vol. 8, no. 3, pp. 239–245, May 2014.
- 824 [112] I. Orović and S. Stanković, “Improved higher order robust distributions based on
825 compressive sensing reconstruction,” *IET Signal Processing*, vol. 8, no. 7, pp. 738–
826 748, September 2014.
- 827 [113] S. Stanković and L.J. Stanković, “Introducing time-frequency distribution with a
828 “complex-time” argument,” *Electronics Letters*, vol. 32, no. 14, pp. 1265–1267, Jul.
829 1996.
- 830 [114] I. Orović and S. Stanković, “A class of highly concentrated time-frequency distri-
831 butions based on the ambiguity domain representation and complex-lag moment,”
832 *EURASIP Journal on Advances in Signal Processing*, vol. 2009, no. 1, p. 935314,
833 2009.
- 834 [115] E. Sejdić, I. Orović, and S. Stanković, “A software companion for compressively
835 sensed time-frequency processing of sparse nonstationary signals,” *SoftwareX*, 2017,
836 under consideration.